Advances in Nano Research, *Vol. 15, No.5 (2023) 423-439*
https://doi.org/10.12989/anr.2023.15.5.423

An analytical study on free vibration of magneto electro micro sandwich beam with FG porous core on Vlasov foundation

Kazem Alambeigi, Mehdi Mohammadimehr* and Mostafa Bamdad

Department of Solid Mechanics, Faculty of Mechanical Engineering, University of Kashan, Kashan, Iran

(*Received November 14, 2021, Revised April 5, 2022, Accepted June 30, 2022*)

Abstract. The aim of this paper is to investigate the free vibration behavior of the micro sandwich beam composing of five layers such as functionally graded (FG) porous core, nanocomposite reinforced by carbon nanotubes (CNTs) and piezomagnetic/ piezoelectric layers subjected to magneto electrical potential resting on silica aerogel foundation. The effect of foundation has been taken into account using Vlasov model in addition to rigid base assumption. For this purpose, an iterative technique is applied. The material properties of the FG porous core and FG nanocomposite layers are considered to vary throughout the thickness direction of the beams. Based on the Timoshenko beam theory and Hamilton's principle, the governing equations of motion for the micro sandwich beam are obtained. The Navier's type solution is utilized to obtain analytical solutions to simply supported micro sandwich beam. Results are verified with corresponding literatures. In the following, a study is carried out to find the effects of the porosity coefficient, porous distribution, volume fraction of CNT, the thickness of silica aerogel foundation, temperature and moisture, geometric parameters, electric and magnetic potentials on the vibration of the micro sandwich beam. The results are helpful for the design and applications of micro magneto electro mechanical systems.

Keywords: FG porous core; micro sandwich beam; nanocomposite; piezomagnetic/piezoelectric layers; porosity; vibration; Vlasov foundation

1. Introduction

1.1 Porous materials

In recent years, modern materials such as functionally graded porous materials (FGPMs) in sandwich structures are noticed from researchers because of vast usage of these materials. Due to their lightness and high strength, porous materials can be a great choice to be used in core of sandwich structures. Free vibration of electro magneto thermo sandwich Timoshenko beam with porous core is investigated by Safari *et al*. (2021). In their contribution, the effect of temperature, porosity distributions, material length scale parameter, and weight fraction of graphene plates on the natural frequency of the structure are investigated. The outcomes indicates that the value of the nano particles has a crucial impact on the structure's stiffness; plus, the escalation of temperature contributes to decline of natural frequency. Kim *et al*. (2018) studied bending, buckling and free vibration of FG porous micro-plates based on first order shear deformation theory (FSDT). They considered the effect of different porosity distributions and micro size effect on behavior of micro porous plate. Al-shujairi and Mollamahmutoğlu (2018) employed nonlocal strain gradient theory for buckling and free vibration analysis of an FG sandwich micro-beam resting on elastic foundation. The effect of different parameters such as nonlocal parameter, aspect ratio and temperature change were investigated. They concluded the nonlocal parameter decreases the stiffness of structures while it is vise versa for material length scale parameter. Kitipornchai *et al*. (2016) employed Timoshenko beam theory to investigate free vibration and elastic buckling of functionally graded (FG) porous beams reinforced by graphene platelets (GPL). They concluded the GPL increases the stiffness of structures. Nejadi *et al*. (2021) studied free vibration and buckling analysis of nanocomposite Timoshenko sandwich beam with porosity core resting on variable elastic foundation. They considered the effect of different parameters such as porosity distribution and porosity coefficient on the stiffness of the beam, and also investigated the effect of volume fraction distribution of fibers, numbers, and angles of layers on natural frequency and critical bucking load.The vibration and stability of a simply supported beam with axially moving motion and spinning motion was studied by Zhu and Chung (2019) using Rayleigh beam theory. They presented the effect of flexure stiffness and rotary inertia factor on the stability boundary. Chan *et al*. (2020) has employed Hamilton's principle to derive the motion equations of a piezoelectric functionally graded porous truncated conical panel, and analyzed the results by Galerkin's and Runge-Kutta methods. In their study, the effect of porosity distribution, porosity coefficient, applied actuator voltage and temperature has been investigated on nonlinear dynamic response and free vibration of functionally graded porous (FGP) panel. The outcome shows the porosity distribution and coefficient have effect on the natural frequencies and deflection amplitudes of the piezoelectric FGP pan, and by elevating the temperature, the deflection will increase as well. Chen *et al*. (2016a) presented the nonlinear free vibration behavior of shear

*Corresponding author, Professor,
E-mail: mmohammadimehr@kashanu.ac.ir

ISSN: 2287-237X (Print), 2287-2388 (Online)

deformable sandwich porous beam within the context of Timoshenko beam theory. Their proposed beam is composed of two face layers and a functionally graded porous core which contains internal pores following different porosity distributions. They applied the Ritz method and von Kármán type nonlinear strain-displacement relationships to derive the equation system. In the other work, they (2016b) illustrated the free and forced vibration characteristics of functionally graded (FG) porous beams with non-uniform porosity distribution whose elastic moduli and mass density are nonlinearly graded along the thickness direction. The relationship between coefficients of porosity and mass density is determined based on the typical mechanical property of an open-cell metal foam. They obtained the natural frequencies and transient dynamic deflections for porous beams under different loading conditions, including a harmonic point load, an impulsive point load and a moving load with constant velocity and investigated the effects of varying porosity distribution, porosity coefficient, slenderness ratio and boundary condition, shedding important insights into the design of functionally graded porous beams to achieve improved dynamic behavior. Wu *et al*. (2020) considered functionally graded porous structures (FGPSs), characterized by a continuous spatial gradient in both porosity and material properties, as the new generation lightweight structures. They investigated in their research that consists of: (i) a brief introduction of porous materials and Functionally graded porous materials (FGPMs); (ii) an elaboration of the key factor and micromechanical models related to material properties of FGPMs; (iii) a comprehensive review of mechanical analysis of FGPSs; (iv) a detailed discussion of the main challenges and future research directions; (v) a conclusion. Chen *et al*. (2017) investigated the nonlinear free vibration and postbuckling behaviors of multilayer functionally graded (FG) porous nanocomposite beams that are made of metal foams reinforced by graphene platelets (GPLs). They found that the addition of a small amount of GPLs can remarkably reinforce the stiffness of the beam, and its nonlinear vibration and postbuckling performance is significantly influenced by the distribution patterns of both internal pores and GPL nanofillers.

1.2 Micro and nano structures as well as FG materials

With the development of the material science and nanotechnology, micro systems are the new field in which FGM or FGPMs have been utilized to achieve the desired performance. Among all micro systems, micro beams have obtained intense attention among researchers since micro beams are a main part of many micro rotors. The dynamic responses of micro scale structural elements created with FG porous materials vary with elements which are constructed with conventional materials in small scale structures. Micro sandwich beams with flexible core are new class of sandwich structure which are efficiently lightweight and high stiffness. Over the past few years, dynamic and static properties of sandwich structures have been investigated by many researchers. However, most of the researches available in open literature did not consider the possible improvement offered by porous distribution across the thickness and multi-field loads to control structural vibrations. Several studies have been carried out on free vibration and static analysis of sandwich structures, micro and nano structures in last years.

Luat *et al*. (2021) presented the mechanical analysis of bi-functionally graded sandwich nanobeams. They investigated the influence of some parameters such as the slender ratio, the power-law index, the skin-core-skin thicknesses and the small-scale parameter on the bending, free vibration and buckling behavior of bi-functionally graded sandwich nanobeams. Arani and Kiani (2018) considered nonlinear free and forced vibration analysis of microbeams resting on the nonlinear orthotropic visco-Pasternak foundation with different boundary conditions. They concluded that the orthotropic visco-Pasternak foundation and various boundary conditions has an important role on the natural and response frequencies. Transient responses of functionally graded double curved shallow shells with temperature-dependent material properties are studied by Duc and Quan (2014). They offered an analytical method to investigate the nonlinear dynamic response and vibration of imperfect eccentrically stiffened FGM double curved thin shallow shells on elastic foundation. They found that the parameters such as initial imperfection, volume fraction index and geometrical affect strongly the nonlinear dynamic response and nonlinear vibration of the FGM shells. Arefi *et al*. (2016) considered free vibration analysis of functionally graded laminated sandwich cylindrical shells integrated with piezoelectric layers. They concluded that the piezoelectric layers and functionally grared material has an important role in this structures. Ebrahimi and Barati 2018 illustrated hygro-thermal vibration analysis of bilayer graphene sheet system via nonlocal strain gradient plate theory. They concluded that hygro-thermal and material lenght scale parameter has a main role on the natural frequency. Using Reddy's third-order shear deformation shell theory, Duc (2016a, b) analyzed nonlinear thermal dynamic of eccentrically stiffened S-FGM circular cylindrical shells surrounded on elastic foundations. The structure is affected by mechanical, damping loads and temperature and the Bubnov–Galerkin method is applied to acquire results. He concluded that temperature, elastic foundations, and outside stiffeners had a significant impact on dynamic response of the S-FGM circular cylindrical shells. Over another study which conducted by this author in the same year on nonlinear thermoelectro-mechanical dynamic response of a functionally graded sandwich circular cylindrical shells, he explored the impact of material properties, imperfection, and thermo-electro-mechanical and damping loads on the nonlinear dynamic response of the shells. Also, an excellent investigations have been carried out on nonlinear static, buckling and postbuckling analysis of shells and panels (Vuong and Duc 2020, Duc and Tung 2010, Khoa *et al*. 2017). They employed Galerkin method and the fourth-order Runge–Kutta method to derive the results which the outcome depicts the effect of material properties, imperfection, and thermo-electro-mechanical and damping

loads on the nonlinear dynamic response of the shells. Khdeir and Aldraihem (2016) studied free vibration of sandwich beams with soft core. Their comparisons showed that the zig-zag theory provides accurate predictions of the natural frequencies for sandwich beams with soft core. Bamdad *et al.* (2020) demonstrated bending and buckling analysis of sandwich Reddy beam considering shape memory alloy wires and porosity resting on Vlasov's foundation. Their obtained results showed that when SMA wires are in martensite phase, the maximum deflection of the sandwich beam decreases and the critical buckling load increases significantly. Madenci (2021) considered free vibration analysis of carbon nanotube RC nanobeams with variational approaches. They employed the rule of mixture to estimate the effective material properties of single-walled CNT reinforced nanobeams. Sadeghpour *et al.* (2015) presented free vibration analysis of a debonded curved sandwich beam. Their results indicated that the fundamental natural frequencies are seriously affected by curvature angle and debond, whereas the higher order natural frequencies showed relatively small changes and concluded that Face/ core debond causes reduction of the natural frequencies. Şimşek and Al-shujairi (2016) presented static, free and forced vibration of functionally graded (FG) sandwich beams excited by two successive moving harmonic loads. At the same time, extensive static and free vibration results are presented to check the reliability of their present formulation. Tossapanon and Wattanasakulpong (2016) presented stability and free vibration of functionally graded sandwich beams resting on two-parameter elastic foundation. They concluded that the elastic foundation increases the stiffness of structures. Walczak *et al.* (2017) investigated buckling and vibrations of metal sandwich beams with trapezoidal corrugated cores – the lengthwise corrugated main core. Their results are compared with these given by the numerical solution realised with the use of the finite element method in the ANSYS and ABAQUS systems. Zhang *et al.* (2017) presented free vibration analysis of sandwich beams with honeycomb-corrugation hybrid cores. For sandwich beams with corrugated cores, the filling honeycomb not only enhances their flexural rigidity and increases their natural frequency of higher orders, but also more or less eliminates the anisotropy of the structural stiffness and suppresses the local modes of vibration. Akhavan Alavi *et al.* (2019) studied optimal active vibration control of a micro sandwich beam. They used modified strain gradient theory to obtain governing equations of motion for smart micro Reddy beam and concluded that the material length scale parameter increases the stiffness of beam structures. Wang *et al.* (2018) investigated vibration response of an FG graphene nano-platelet reinforced composite (FG-GPLRC) beam under two successive moving masses. They also, proposed a new high order shear deformation theory (HSDT) to analyze the structural behavior of FG-GPLRC beams. The nonlocal theory was employed for vibration analysis of FG Timoshenko beam by Zhang *et al.* (2018). Their results indicated that nonlocal parameters play an important role on vibration behavior of nanobeam and the increase of the nonlocal parameters leads to the decrease of the frequency as well. Domagalski (2018) implemented Rayleigh theory to study large amplitude vibrations of periodically inhomogeneous slender beams. Their results of nonlinear vibrations analysis are presented by backbone and amplitude-frequency response curves, time series, Poincare sections and bifurcation diagrams. Experimental vibration analysis of composite sandwich beams with magneto-rheological honeycomb core was studied by Souza *et al.* (2018). They concluded that magnetorheological honey-comb core has a important role on the natural frequency. Vibration analysis of micro beam and micro plate with various kinds of boundary conditions was performed by Ansari *et al.* (2017) by using a 3D finite element approach. Also, their results of MPT are compared with those of classical theory and it is indicated that there is a considerable difference between their predictions at small scales. Dastjerdi and Abbasi (2018) used a torsional spring to model a crack on micro beam in order to study bending and vibration characteristics of the beam. Their results indicate that the frequency and sensitivity would be maximum when the crack is approximately in the middle of the cantilever. Growing the crack size can result in the variations of either resonant frequency or sensitivity especially for more stiff samples. Vibration analysis has brought a special charm for many researchers around the world due to their vital role in condition monitoring of various types of mechanical structures. In bygone years, a large number of scientists investigated both linear and nonlinear vibration response on sandwich plates and shells (Quan and Duc 2016, Duc and Tung 2010, Duc and Pham 2021, Quan *et al.* 2020, Mohammadimehr 2022, Safari *et al.* 2023). She *et al.* (2018) studied vibration behavior of porous nanotube. They investigated the effects of the nonlocal parameter, porosity volume fraction, strain gradient parameter, temperature variations and material variation on vibration behavior of the nanotubes. Sahmani *et al.* (2018) investigated nonlinear vibrational behavior of FG porous micro plates reinforced with GPLs. They concluded that the considering GPL leads to increase the stiffness of structures. Modified couple stress theory was employed for the vibration analysis of two-dimensional FG micro beam made of porous material by Mirjavadi *et al.* (2018). They indicated that increment of temperature change leads to decrease the nondimensional frequency. Quan *et al.* (2021) and Dat *et al.* (2020) studied an analytical method for nonlinear thermos-electro-magneto vibration of a plates. In their contribution, the influence of elastic foundations, geometrical parameters, temperature and moisture on the nonlinear vibration of the plate are investigated. The results illustrate that elastic foundations has a positive effect and temperature and moisture have a negative influence. Xue *et al.* (2019) implemented FSDT to study free vibration behaviors of porous plates which have porosity distributions in both thickness and in-plane directions. They investigated the effect of important parameters including porosity coefficient, geometric parameters and boundary conditions on free vibration of porous plates. Liu *et al.* (2018) presented vibration analysis of an FG magneto-electro-viscoelastic nanobeam resting on the visco-Pasternak foundation. They used nonlocal Timoshenko beam theory

combining with the Kelvin-Voigt viscoelastic model to derive governing equations. Size-dependent nonlinear free vibration behavior of porous beam with an initial geometrical curvature was investigated by Li *et al.* (2017). They explored the effect of the dispersion patterns of porosities, the vibration amplitude and geometric imperfection on the nonlinear vibration of porous beam. Akbaş (2017) used finite element method to study forced vibration of an FG porous deep beam under dynamically load. The results demonstrated that porosity has an important effect on the dynamic responses of the FG porous deep beam. Bahaadini and Saidi (2018) investigated vibration and stability of spinning FG thin-walled porous beams reinforced by GPLs subjected to compressive axial load. They concluded that the considering GPL leads to increase natural frequency. A semi-analytical model for free vibration analysis of rotating FG material beams with porosities and double tapered cross section was presented by Tian *et al.* (2018). Their results illustrated that some parameters such as rotation speed and porosity volume fraction have remarkable effect on vibration behavior of porous rotating functionally graded material (FGM) beam. Zeng *et al.* (2018) studied nonlinear vibration of piezoelectric sandwich nanoplates with an FG porous core subjected to electrical load. Their results indicated that the natural frequency of the sandwich structure with porous core is adjustable by controlling the porous coefficients and porosity distribution of the core. Eltaher *et al.* (2018) developed a modified porosity model to analyze bending and vibration of porous FGM nanobeams. They used nonlocal stress theory and Euler beam theory to investigate vibration of porous FGM nanobeams and concluded that the nonlocal parameter decreases the natural frequency and vice versa for deflection. Nguyen *et al.* (2019) presented the modeling and analysis for mechanical response of nano-scale beams undergoing large displacements and rotations that they modeled the beam element as a composite consisting of the bulk material and the surface material layer. Also. they considered both Eringen nonlocal elasticity theory and Gurtin–Murdoch surface elasticity theory to formulate the moment–curvature relationship of the beam. They demonstrated that the proposed technique yields highly accurate results comparable to the benchmark analytical solutions. In addition, they concluded that the nonlocal and surface energy effects play a significant role on the predicted buckling load, post-buckling and bending responses of the nano-beam. In particular, the presence of those effects remarkably alters the overall stiffness of the beam and predicted solutions exhibit strong size-dependence when the characteristic length of the beam is comparable to the intrinsic length scale of the material surface. Tran *et al.* (2020) reported the analytical free-vibration analysis of a stiffened functionally graded circular cylindrical shell resting on a Winkler–Pasternak foundation and considered various boundary conditions and the thermal effect. They assumed the material properties to be temperature-dependent and vary continuously across the shell's thickness according to the power law distribution of the volume fraction of constituents. In their numerical investigations, the influence of temperature field, material volume fraction index, elastic foundation coefficients, boundary conditions, and geometrical ratios on the fundamental natural frequencies of the shell is also given and discussed. Sae-Long *et al.* (2021a) presented a novel flexibility-based beam-foundation model for inelastic analyses of beams resting on Winkler-Pasternak foundation model. Through equilibrated force shape functions, they related the internal force fields to the element force degrees of freedom. and adopted Tonti's diagrams to present both strong and weak forms of the problem. They employed three numerical simulations to assess validity and to show effectiveness of the proposed flexibility-based beam-foundation model. The influences of the adopted foundation model to represent the underlying foundation medium are also discussed. In the other work, they (2021b) developed a rational beam-elastic substrate model with inclusion of nonlocal and surface-energy effects for bending and buckling analyses of nanobeams lying on elastic substrate media. They employed the thermodynamics-based strain gradient theory to represent the beam-bulk nonlocality while the Gurtin–Murdoch surface theory is utilized to account for the surface-free energy. Interaction between the beam and its underlying substrate medium is described by the Winkler foundation model. Vo *et al.* (2022a) developed a new 2D field-consistent Euler-Bernoulli beam element for the analysis of beam structures undergoing large displace-ments but small strains. They derived the relationships between the cross-sectional rotation and displacements of the beam axis, and consequently, the kinematics of the element are entirely described by the displacements of the beam axis. For better geometric representations of complex deformed configurations, some of the weights are treated as discrete unknowns. Several benchmark numerical examples are used to demonstrate the accuracy and robustness of the proposed beam element. The merits of considering weights as discrete unknowns are verified through comparisons between elements having varying weights and stationary weights. Furthermore, their proposed beam element is found to be naturally free from membrane locking, and thus, no additional efforts are required to handle the locking issues.Long *et al.* (2022) presented an exact solution for nonlinear static behaviors of functionally graded (FG) beams with porosities resting on the elastic foundation. By contrast, in their study, the physical neutral surface of the beam is utilized. Based on the Timoshenko beam theory, von Kármán nonlinear assumption, together with neutral surface concept, they derived the nonlinear governing equations of the FG beam resting on the elastic foundation. They conducted the exact solution for the problem with all immovable and moveable boundary conditions in detail. Some numerical investigations to show the effects of boundary conditions, material properties, length-to-thickness ratio, elastic foundation coefficients and several types of applied load on nonlinear static bending behaviors of the beam are given. Vo *et al.* (2022b) considered spatial arbitrarily curved microbeams with the modified couple stress theory. The moving trihedron of the beam axis are used to form a local Cartesian coordinate system. Displace-ments of the beam axis and cross-sectional rotations in the local coordinate system are considered as unknowns in the

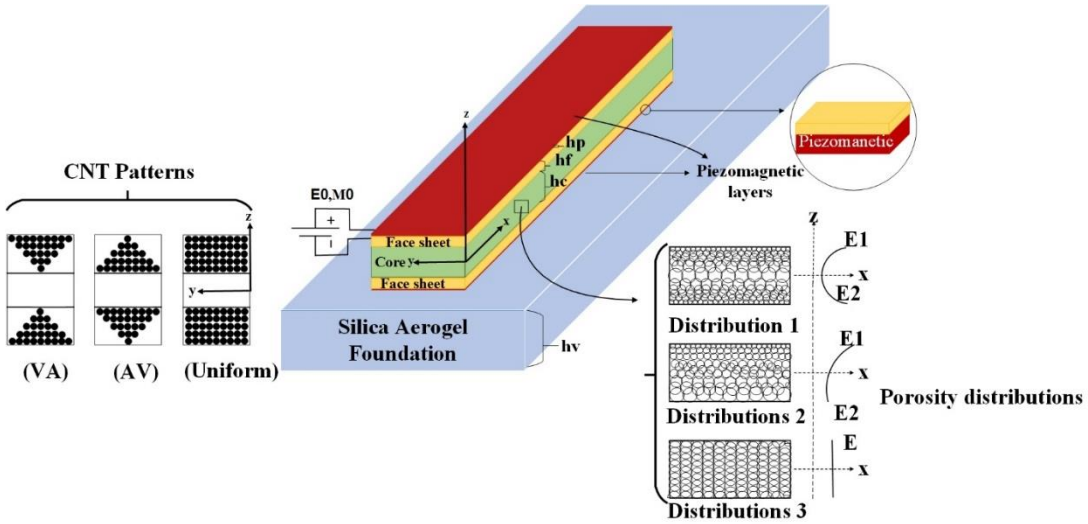

Fig. 1 A schematic view of micro sandwich beam on Vlasov substrate under magnetic and electric fields

kinematic descriptions. They used the principle of virtual work to derive the equations of motion. The accuracy of the derived equations of motion is tested by a comparison with existing studies of planar circular and straight microbeams. Since this is the first study for the use of the modified couple stress theory in the setting of spatial arbitrarily curved microbeams, the outputs of the present study enable further in-deep analysis to comprehend these structures.

A review of the literature shows that vibration analysis of micro sandwich beam with functionally graded porous core subjected to electric and magnetic field on Vlasov Foundation (resting on silica aerogel foundation) has not been investigated. The motivations and practical applications of this kind of sandwich beam resting on silica aerogel foundation becomes for increasing stiffness of micro structure using varying the thickness of these foundation. Further, as far as the authors know, there is no reported work on the free vibration of FG sandwich beam with five layers and porous core under the electric and magnetic potentials. In the present study, the free vibration analysis of FG sandwich beam with porous core subjected to electric and magnetic potentials and also temperature and moisture change is studied by using Timoshenko beam theory (TBT). It is assumed that in FG part of the sandwich beam the material properties vary continuously through the thickness of the beam. The equations of the motion are obtained by using the Hamilton's principles and solved via Navier's method. In this study, the effects of the different important parameters such as porosity coefficient, CNT distribution pattern, temperature change and electric and magnetic potentials on the vibration behavior of sandwich beams are discussed.

2. Modeling of problem and formulations

Consider a micro sandwich beam composing of five layers such as two nanocomposites reinforced by carbon nanotubes layers, functionally graded porous core and two piezomagnetic/piezoelectric layers subjected to magneto electrical loadings resting on silica aerogel foundation as shown in Fig. 1. The length and width of micro beam are L and b, respectively, and h_c, h_f and h_p denote thicknesses of core, composite layers and piezomagnetic layers, respectively. Various porosity distributions include uniform distribution (UD) and porosity distribution 1 and 2 are illustrated in this figure. Also, Fig. 1. shows in a Cartesian coordinate that x-axis is in the length direction and z-axis is in the thickness direction. Two methyl methacrylate (PMMA) face layers reinforced by three different carbon nanotubes patterns are face sheets and two piezomagnetic layers are subjected to magneto electro elastic loads.

The advantage of sandwich model in the present work is stated as follows:

By employing a sandwich model not only the total weight of a structure can be loss but the structure can be stiffened as well. In this work, a porous core has been considered to reduce the weight and stiff composite layers are applied to enhance the stiffness of the structure. In sandwich structures, researchers are looking to increase the high strength to weight ratio.

The disadvantage of sandwich structure has been considered as:

Making a coupling between these layers would be a serious issue in practice because in vibration discussion, the sandwich beam model is assumed to be as a continuous body that no delamination occurs between the layers of these sandwich structure.

2.1 Material properties of porous core

Three different porosity distributions in the core including non-uniform FG porosity and uniform distributions as shown in Fig. 1, resulting in position-dependent variations of Young's modulus $E_c(z)$, shear modulus $G_c(z)$ and mass density $\rho_c(z)$, described by Eq. (1) for distribution 1 (symmetric distribution), Eq. (2) for distribution 2 (asymmetric distribution) and Eq. (3) for uniform distribution (Kiarasi *et al*. 2021, Nejadi and Mohammadimehr 2020):

$$\begin{cases} E_c(z) = E_1^c\left(1 - e_0 cos(\pi\xi)\right), \\ G_c(z) = \dfrac{E_c(z)}{2(1+\upsilon_c(z))}, \rho_c(z) = \rho_1^c\left(1 - e_m cos(\pi\xi)\right) \end{cases} \quad (1)$$

$$\begin{cases} E_c(z) = E_1^c\left(1 - e_0 cos\left(\dfrac{\pi\xi}{2} + \dfrac{\pi}{4}\right)\right), \\ G_c(z) = \dfrac{E_c(z)}{2\left(1+\upsilon_c(z)\right)}, \\ \rho_c(z) = \rho_1^c\left(1 - e_m cos\left(\dfrac{\pi\xi}{2} + \dfrac{\pi}{4}\right)\right) \end{cases} \quad (2)$$

$$\begin{cases} E_c(z) = E_1^c(1 - e_0\,\lambda), \quad G_c(z) = \dfrac{E_c(z)}{2\left(1+\upsilon_c(z)\right)}, \\ \rho_c(z) = \rho_1^c\sqrt{1 - e_0\,\lambda} \end{cases} \quad (3)$$
$$\lambda = \frac{1}{e_0} - \frac{1}{e_0}\left(\frac{2}{\pi}\sqrt{1-e_0} - \frac{2}{\pi} + 1\right)^2$$

$$\begin{aligned} &\upsilon_c(z) = 0.221p' + \upsilon_1\left(0.342p'^2 - 1.21p' + 1\right), \\ &p' = 1 - \left(\frac{\rho_c(z)}{\rho_1^c}\right) \end{aligned} \quad (4)$$

where ξ is $\frac{z}{h_c}$, E_1^c and ρ_1^c are values of Young's modulus and mass density of the pure metal core, respectively. e_0 is defined as the principal coefficient to describe the porosity. Larger value of porosity coefficient leads to a lower elastic modulus and its range is between 0 to 1. $e_m$is the porosity coefficient for mass density and can be calculated like below:

$$e_0 = 1 - \frac{E_2}{E_1} \quad (5)$$

$$e_m = 1 - \sqrt{1 - e_0} \quad (6)$$

where E_2 and E_1 are minimum and maximum values of Young's modulus of porous core, respectively.

2.2 Material properties of nanocomposite

In present study, the composite layers of the micro sandwich beam are made from poly methyl methacrylate as matrix of the composite reinforced by functionally graded distributions of CNTs that the composite layer is anisotropic. The rule of mixture is utilized to obtain the mechanical properties of CNT reinforced composite layers as follows (Mohammadimehr *et al*. (2017, 2018)):

$$E_f = \eta_1 V^{CNT} E_{11}^{CNT} + V^{PMMA} E^{PMMA} \quad (7)$$

$$\rho_f = V^{CNT}\rho^{CNT} + V^{PMMA}\rho^{PMMA} \quad (8)$$

$$\nu_f = V^{CNT}\nu^{CNT} + V^{PMMA}\nu^{PMMA} \quad (9)$$

where $\eta_1 = 0.137$ is the efficiency parameter, ρ and ν represent density and Poisson's ratio for CNT, PMMA, respectively, and f are used to describe carbon nanotube and polymethyl methacrylate matrix and composite, respectively.

E_{11}^{CNT} and E^{PMMA} are Young's modulus of CNT and Young's modulus of PMMA matrix, respectively. V^{CNT} and V^{PMMA} denote volume fraction of CNT and PMMA matrix, respectively. CNT volume fraction can be calculated as Eq. (10) due to the three different CNT distributions along the thickness of composite layer, and PMMA volume fraction can be calculated as $V_{PMMA} = 1 - V_{CNT}$.

$$V_{CNT} = \begin{cases} V_{CNT}^t = \dfrac{2z - h_c}{h_f} V* \\ V_{CNT}^b = \dfrac{2z + h_c}{-h_f} V* \end{cases} \rightarrow Pattern: VA$$

$$V_{CNT} = \begin{cases} V_{CNT}^t = V* \\ V_{CNT}^b = V* \end{cases} \rightarrow Pattern: Uniform \quad (10)$$

$$V_{CNT} = \begin{cases} V_{CNT}^t = \dfrac{h_c + 2h_f - 2z}{h_f} V* \\ V_{CNT}^b = \dfrac{h_c + 2h_f + 2z}{h_f} V* \end{cases} \rightarrow Pattern: AV$$

where $V*$ is the volume fraction of CNT. h_c and h_f are the thichnesses of core and facesheets, respectively.

The weight fraction of CNT nanofillers (W_{CNT}) is related to its volume fraction ($V*$) by Eq. (11) (Mohammadimehr *et al*. 2016a, b):

$$V* = \frac{W_{CNT}}{W_{CNT} + \frac{\rho_{CNT}}{\rho_{PMMA}} - \frac{\rho_{CNT}}{\rho_{PMMA}} W_{CNT}} \quad (11)$$

where ρ_{CNT} and ρ_{PMMA} are the mass density for CNT and PMMA, respectively.

2.3 Theoretical formulations

The displacement fields of the Timoshenko beam theory are assumed to be as follows (Mohammadimehr *et al*. (2018)):

$$\begin{aligned} u_X^i(x,z,t) &= u_0^i(x,t) + z\phi^i(x,t) \\ w_Z^i(x,z,t) &= w_0^i(x,t) \end{aligned} \quad (12)$$

In Eq. (12), $u_x^i (i = c, tf, bf, tp, bp)$ and w_z^i denote the displacements of Timoshenko beam in the x and z directions, respectively, superscripts c, tf, bf, tp, bp denote core, top composite layer, bottom composite layer, top piezomagnetic layer and bottom piezo magnetic layer, respectively. u_0^i and w_0^i denote the axial and transverse displacements of the beam mid-plane, respectively. ϕ^i represents the transverse normal rotation about the *z*-axis, and t is the time.

The axial and transverse shear strains based on linear strain-displacement relationship are written as follows:

$$\varepsilon_{XX}^i = \frac{\partial u_0^i}{\partial x} + z\frac{\partial \phi^i}{\partial x} \rightarrow (i = c, tf, bf, tp, bp) \quad (13)$$

$$\gamma_{XZ}^i = \phi^i + \frac{\partial w_0^i}{\partial x} \rightarrow (i = c, tf, bf, tp, bp) \quad (14)$$

Using linear stress-strain constitutive law, the normal stress and transverse stress of the porous core, composite

Table 1 Material properties of piezomagnetic

C_{11}	$226(GPa)$
C_{55}	$44.2(GPa)$
e_{31}	-2.2 (C/m^2)
e_{15}	-2.2 (C/m^2)
k_{11}	5.64 (10^{-9}) (Ns/CV)
k_{33}	6.35 (10^{-9}) (Ns/CV)
q_{31}	290 (N/Am)
q_{15}	290 (N/Am)
d_{11}	5.367(10^{-12}) (Ns/CV)
d_{33}	5.367(10^{-12}) (Ns/CV)
g_{11}	297(10^{-6}) (Ns^2/C^2)
g_{33}	82.3(10^{-6}) (Ns^2/C^2)
$\rho_{pizomagnetic}$	5550 (Kg/m^3)

layers and piezomagnetic layers can be written as Eqs. (15)-(17) (Mohammadimehr *et al*. 2016b):

$$\begin{Bmatrix}\sigma_{XX}\\ \tau_{XZ}\end{Bmatrix}^c = \begin{bmatrix}c_{11} & 0\\ 0 & c_{55}\end{bmatrix}^c \begin{Bmatrix}\varepsilon_{XX}-\alpha_c\Delta T-\beta_c\Delta C\\ \gamma_{XZ}\end{Bmatrix}^c \tag{15}$$

$$\begin{Bmatrix}\sigma_{XX}\\ \tau_{XZ}\end{Bmatrix}^f = \begin{bmatrix}c_{11} & 0\\ 0 & c_{55}\end{bmatrix}^f \begin{Bmatrix}\varepsilon_{XX}-\alpha_f\Delta T-\beta_f\Delta C\\ \gamma_{XZ}\end{Bmatrix}^f (f=tf,bf) \tag{16}$$

$$\begin{Bmatrix}\sigma_{XX}\\ \tau_{XZ}\end{Bmatrix}^p = \begin{bmatrix}c_{11} & 0\\ 0 & c_{55}\end{bmatrix}^p \begin{Bmatrix}\varepsilon_{XX}-\alpha_p\Delta T-\beta_p\Delta C\\ \gamma_{xz}\end{Bmatrix}^p - \begin{bmatrix}0 & e_{31}\\ e_{15} & 0\end{bmatrix}^p \begin{Bmatrix}E_x\\ E_Z\end{Bmatrix}^p - \begin{bmatrix}0 & q_{31}\\ q_{15} & 0\end{bmatrix}^p \begin{Bmatrix}M_X\\ M_Z\end{Bmatrix}^p (p=tp,bp) \tag{17}$$

where α, β, ΔT, ΔC indicate thermal expansion coefficient, moisture coefficient, temperature changes, and moisture changes, respectively. σ_{XX} and τ_{XZ} are the normal and shear stresses, respectively. E_x and E_z are the electric fileds in the x and z directions, respectively. M_x and M_z denote the magnetic fields in the x and z directions, respectively. e_{31} and e_{15} are the piezoelectric constants. Also, q_{31} and q_{15} denote the piezomagnetic constants. Elastic stiffness (c_{11}, c_{55}) of porous core and composite layers are given as Eqs. (18) and (19) and elastic coefficient of piezomagnetic layers are given in Table 1.

$$c_{11}^i(z) = \frac{E^i(z)}{1-(\nu^i)^2}(i=c,tf,bf) \tag{18}$$

$$c_{55}^i = \frac{E^i(z)}{2(1+\nu^i)}(i=c,tf,bf) \tag{19}$$

Piezomagnetic constants are assumed as Arefi *et al*. (2018) in Table 1.

Based on the modified couple stress theory, the components of the symmetric curvature tensor are defined as the following form (Akhavan Alavi *et al*. 2019):

$$\chi_{12} = \frac{1}{2}(\frac{\partial\theta_1}{\partial y}-\frac{\partial\theta_2}{\partial x}), \chi_{13} = \frac{1}{2}(\frac{\partial\theta_1}{\partial z}-\frac{\partial\theta_3}{\partial x}), \chi_{23} = \frac{1}{2}(\frac{\partial\theta_2}{\partial z}-\frac{\partial\theta_3}{\partial y}) \tag{20}$$

where χ_{ij} is the components of symmetric rotation gradient tensor and θ is the components of the rotation vector that can be expressed as follows (Akhavan Alavi *et al*. 2019):

$$\theta_1 = \frac{1}{2}\left(\frac{\partial w}{\partial y}-\frac{\partial v}{\partial z}\right), \theta_2 = \frac{1}{2}\left(\frac{\partial u}{\partial z}-\frac{\partial w}{\partial x}\right), \theta_3 = \frac{1}{2}(\frac{\partial v}{\partial x}-\frac{\partial u}{\partial y}) \tag{21}$$

The components of the couple stress tensor are considered as follows:

$$m_{12} = 2Gl_m^2\chi_{12}, m_{13} = 2Gl_m^2\chi_{13}, m_{23} = 2Gl_m^2\chi_{23} \tag{22}$$

where m_{ij} is the components of symmetric couple stress tensor. and G and $l_m$are the shear modulus and material length scale parameter, respectively.

In Eq. (17), e and q represent piezoelectric and piezomagnetic constants. The distribution of electric and magnetic potentials along the thickness direction is supposed to be changed as a combination of a cosine and linear variation as Eq. (23) and Eq. (24) respectively (Arefi and Zenkour 2017):

$$\begin{cases}\psi(x,z,t) = -cos\left(\frac{\pi\left(z-\frac{\hbar c}{2}-\hbar f\right)}{\hbar p}\right)E(x,t)\\ +2\frac{(z-\frac{\hbar c}{2}-\hbar f)}{\hbar p}E_0\frac{\hbar c}{2}+\hbar f<z<\frac{\hbar c}{2}+\hbar f+\hbar p\\ \psi(x,z,t) = -cos\left(\frac{\pi\left(-z-\frac{\hbar c}{2}-\hbar f\right)}{\hbar p}\right)E(x,t)\frac{-\hbar c}{2}\\ -\hbar f-\hbar p<z<\frac{-\hbar c}{2}-\hbar f\end{cases} \tag{23}$$

$$\begin{cases}\Gamma(x,z,t) = -cos\left(\frac{\pi\left(z-\frac{\hbar c}{2}-\hbar f\right)}{\hbar p}\right)M(x,t)\\ +2\frac{\left(z-\frac{\hbar c}{2}-\hbar f\right)}{\hbar p}M_0\frac{\hbar c}{2}+\hbar f<z<\frac{\hbar c}{2}+\hbar f+\hbar p\\ \Gamma(x,z,t) = -cos\left(\frac{\pi\left(-z-\frac{\hbar c}{2}-\hbar f\right)}{\hbar p}\right)M(x,t)\frac{-\hbar c}{2}\\ -\hbar f-\hbar p<z<\frac{-\hbar c}{2}-\hbar f\end{cases} \tag{24}$$

E_0 and M_0 are the applied electric and magnetic potentials, respectively. $\psi(x,z,t)$ and $\Gamma(x,z,t)$ are the electric and magnetic potentials, respectively. According to electric and magnetic potentials, the components of electric and magnetic fields can be obtained as (Mohammadimehr *et al*. 2016b, Arefi and Zenkour (2017):

$$\begin{cases}E_z = -\frac{\partial\psi}{\partial z} = -\frac{sin\left(\frac{\pi\left(z-\frac{\hbar c}{2}-\hbar f\right)}{\hbar p}\right)\pi E(x,t)}{\hbar p}\\ -\frac{2E_0}{\hbar p}\frac{\hbar c}{2}+\hbar f<z<\frac{\hbar c}{2}+\hbar f+\hbar p\\ E_x = -\frac{\partial\psi}{\partial x} = \cos(\frac{\pi\left(z-\frac{\hbar c}{2}-\hbar f\right)}{\hbar p})(\frac{\partial}{\partial x}E(x,t))\frac{\hbar c}{2}\\ +\hbar f<z<\frac{\hbar c}{2}+\hbar f+\hbar p\end{cases} \tag{25}$$

$$\begin{cases} E_z = -\dfrac{\partial \psi}{\partial z} = \dfrac{sin\left(\dfrac{\pi\left(-z-\frac{\hbar c}{2}-\hbar f\right)}{\hbar p}\right)\pi E(x,t)}{\hbar p} \\ \quad -\dfrac{\hbar c}{2}-\hbar f-\hbar p < z < -\dfrac{\hbar c}{2}-\hbar f \\ E_x = -\dfrac{\partial \psi}{\partial x} = \cos\left(\dfrac{\pi\left(-z-\frac{\hbar c}{2}-\hbar f\right)}{\hbar p}\right)\left(\dfrac{\partial}{\partial x}E(x,t)\right) \\ \quad -\dfrac{\hbar c}{2}-\hbar f-\hbar p < z < -\dfrac{\hbar c}{2}-\hbar f \end{cases} \tag{26}$$

$$\begin{cases} M_z = -\dfrac{\partial \Gamma}{\partial z} = -\dfrac{sin\left(\dfrac{\pi\left(z-\frac{\hbar c}{2}-\hbar f\right)}{\hbar p}\right)\pi M(x,t)}{\hbar p} \\ \quad -\dfrac{2M_0}{\hbar p}\dfrac{\hbar c}{2}+\hbar f < z < \dfrac{\hbar c}{2}+\hbar f+\hbar p \\ M_x = -\dfrac{\partial \Gamma}{\partial x} = \cos\left(\dfrac{\pi\left(z-\frac{\hbar c}{2}-\hbar f\right)}{\hbar p}\right)\left(\dfrac{\partial}{\partial x}M(x,t)\right)\dfrac{\hbar c}{2} \\ \quad +\hbar f < z < \dfrac{\hbar c}{2}+\hbar f+\hbar p \end{cases} \tag{27}$$

$$\begin{cases} M_z = -\dfrac{\partial \Gamma}{\partial z} = \dfrac{sin\left(\dfrac{\pi\left(-z-\frac{\hbar c}{2}-\hbar f\right)}{\hbar p}\right)\pi M(x,t)}{\hbar p} \\ \quad -\dfrac{\hbar c}{2}-\hbar f-\hbar p < z < -\dfrac{\hbar c}{2}-\hbar f \\ M_x = -\dfrac{\partial \Gamma}{\partial x} = \cos\left(\dfrac{\pi\left(-z-\frac{\hbar c}{2}-\hbar f\right)}{\hbar p}\right)\left(\dfrac{\partial}{\partial x}M(x,t)\right) \\ \quad -\dfrac{\hbar c}{2}-\hbar f-\hbar p < z < -\dfrac{\hbar c}{2}-\hbar f \end{cases} \tag{28}$$

The constitutive equations for piezomagnetic layers under electric and magnetic displacements can be expressed as follows:

$$\begin{Bmatrix} D_X \\ D_Z \end{Bmatrix} = \begin{bmatrix} 0 & e_{15} \\ e_{31} & 0 \end{bmatrix}^p \begin{Bmatrix} \varepsilon_{XX} - \alpha_p \Delta T - \beta_p \Delta C \\ \gamma_{XZ} \end{Bmatrix} + \begin{bmatrix} d_{11} & 0 \\ 0 & d_{33} \end{bmatrix}^p \begin{Bmatrix} M_X \\ M_Z \end{Bmatrix} + \begin{bmatrix} k_{11} & 0 \\ 0 & k_{33} \end{bmatrix}^p \begin{Bmatrix} E_X \\ E_Z \end{Bmatrix} (p = tp, bp) \tag{29}$$

$$\begin{Bmatrix} B_X \\ B_Z \end{Bmatrix} = \begin{bmatrix} 0 & q_{15} \\ q_{31} & 0 \end{bmatrix}^p \begin{Bmatrix} \varepsilon_{XX} - \alpha_p \Delta T - \beta_p \Delta C \\ \gamma_{XZ} \end{Bmatrix} + \begin{bmatrix} g_{11} & 0 \\ 0 & g_{33} \end{bmatrix}^p \begin{Bmatrix} M_X \\ M_Z \end{Bmatrix} + \begin{bmatrix} d_{11} & 0 \\ 0 & d_{33} \end{bmatrix}^p \begin{Bmatrix} E_X \\ E_Z \end{Bmatrix} (p = tp, bp) \tag{30}$$

where D_X and D_z are the electric displacements and B_X and B_z denote the magnetic displacements.

The advantage of Vlasov model in the present work is stated as follows:

Vlasov model is considered the shear interactions in a elastic foundation and formulated their problems by using a variational method and solved by iterative technique. This model has been broadly employed by researchers and widely applied to design the structures upon soil foundations. The important merit of the model is that it provides a rigorous theoretical basis for the form of the transverse displacement. Also, in this model, the thickness and material properties (Young's modulus and Poisson's ratio) are considered and based on type of foundation, it can be changed.

The disadvantage of Vlasov model in the present work is stated as follows:

This model due to its variability along thickness and dependence to transverse displacement, it may increase the computing time with employing iterative technique.

Based on Vlasov's model foundation, the foundation parameters can be calculated from geometry and material properties of foundation. The displacement fields of the foundation are considered as (Arani and Zamani 2019):

$$\begin{aligned} u_V(x,z,t) &= 0 \\ w_V(x,z,t) &= w(x,t)\, S(z) \end{aligned} \tag{31}$$

where $w(x,t)\ and\ S(z)$ are transverse deflection in mid-surface of micro beam and shape function of foundation with following boundary conditions:

$$S(-h_v) = 0\,, S(0) = 1 \tag{32}$$

h_v is the thickness of the foundation. According to Arani and Zamani (2019), the shape function of foundation can be considered as:

$$S(z) = \frac{sinh\,\gamma\,(1-\frac{z}{h_v})}{sinh\,\gamma} \tag{33}$$

and γ is calculated by:

$$\gamma^2 = h_v^2 \frac{(1-2\upsilon_{foundation})\int_0^L \left(\frac{dw}{dx}\right)^2 dx}{2(1-\upsilon_{foundation})\int_0^L w^2\, dx} \tag{34}$$

$$\begin{aligned} K_1 &= \int_0^{h_v} \frac{E_{foundation}}{2(1+\upsilon_{foundation})} s(z)^2\, dz \\ K_2 &= \int_0^{h_v} \frac{E_{foundation}(1-\upsilon_{foundation})}{(1+\upsilon_{foundation})(1-2\upsilon_{foundation})} \left(\frac{ds(z)}{dz}\right)^2 dz \end{aligned} \tag{35}$$

For solving Eqs. (33) and (34), it is chosen an initial solution for $\gamma = 1$, and $\gamma_n = 0.01$ in an iterative loop, firstly, the value of $\gamma_n$is equal to γ, then the transverse displacement is placed into Eq. (34) and the new γ is obtained that it is considered for γ_n, this procedure is repeated until some convergence criterion is satisfied $(|\gamma - \gamma_n| < 0.001)$.

Based on the described displacement field of foundation, the strains components can be derived as:

$$\varepsilon_{XX}^v = \frac{\partial u_v}{\partial x} = 0 \tag{36}$$

$$\varepsilon_{ZZ}^v = \frac{\partial w_v}{\partial z} = \frac{\partial S(z)}{\partial z} w(x,t) \tag{37}$$

$$\gamma_{XZ}^v = \frac{\partial u_v}{\partial z} + \frac{\partial w_v}{\partial x} = \frac{\partial w}{\partial x} S(z) \tag{38}$$

$$\begin{Bmatrix} \sigma_{XX} \\ \sigma_{ZZ} \\ \tau_{XZ} \end{Bmatrix}^v = \begin{bmatrix} c_{11} & c_{12} & 0 \\ c_{12} & c_{11} & 0 \\ 0 & 0 & c_{55} \end{bmatrix}^v \begin{Bmatrix} \varepsilon_{XX} \\ \varepsilon_{ZZ} \\ \gamma_{XZ} \end{Bmatrix}^v \tag{39}$$

The Hamilton's principle can be expressed in the

following form to obtain the governing equations of motion.

$$\int_{-\frac{hc}{2}-hf-hp}^{\frac{hc}{2}+hf+hp} (\delta T - \delta U - \delta W)\,dt = 0 \tag{40}$$

In which U is strain energy, T is kinetic energy and W is work done due to the external force.

Strain energy of micro sandwich beam can be calculated as follow (Mohammadimehr *et al*. 2016a, b):

$$\begin{aligned}
&\int_{toppiezo} (\sigma_{xx}^{tp}\delta\varepsilon_{xx}^{tp} + \tau_{xz}^{tp}\delta\gamma_{xx}^{tp} + m_{xy}\delta\chi_{xy} + m_{yz}\delta\chi_{yz} \\
&\qquad - D_Z\delta E_Z - D_X\delta E_X - B_Z\delta H_Z \\
&\qquad - B_X\delta H_X)dv \\
&+ \int_{topcomposite} (\sigma_{xx}^{tf}\delta\varepsilon_{xx}^{tf} + \tau_{xz}^{tf}\delta\gamma_{xx}^{tf} + m_{xy}\delta\chi_{xy} \\
&\qquad + m_{yz}\delta\chi_{yz})dv \\
&+ \int_{core} (\sigma_{xx}^{c}\delta\varepsilon_{xx}^{c} + \tau_{xz}^{c}\delta\gamma_{xx}^{c} + m_{xy}\delta\chi_{xy} + m_{yz}\delta\chi_{yz})dv \\
&+ \int_{\substack{bottom\\composite}} (\sigma_{xx}^{bf}\delta\varepsilon_{xx}^{bf} + \tau_{xz}^{bf}\delta\gamma_{xx}^{bf} + m_{xy}\delta\chi_{xy} \\
&\qquad + m_{yz}\delta\chi_{yz})dv \\
&+ \int_{\substack{bottom\\piezo}} (\sigma_{xx}^{bp}\delta\varepsilon_{xx}^{bp} + \tau_{xz}^{bp}\delta\gamma_{xx}^{bp} + m_{xy}\delta\chi_{xy} + m_{yz}\delta\chi_{yz} \\
&\qquad - D_Z\delta E_Z - D_X\delta E_X - B_Z\delta H_Z \\
&\qquad - B_X\delta H_X)dv
\end{aligned} \tag{41}$$

It is shown the stain components for Vlasov's foundation is obtained from Eqs. (36)-(38), also, the constitutive equations for these elastic foundation has been shown in Eq. (39), thus the strain energy for this foundation is written as follows:

$$\int_{\substack{Vlasov\\foundation}} (\sigma_{xx}^{v}\delta\varepsilon_{xx}^{v} + \sigma_{zz}^{v}\delta\varepsilon_{zz}^{v} + \tau_{xz}^{v}\delta\gamma_{xx}^{v})dv \tag{42}$$

Variation of kinetic energy for micro sandwich beam can be formulated as:

$$\begin{aligned}
&\int_{toppiezo} \rho_p(z)(\dot{u}\delta\dot{u} + \dot{w}\delta\dot{w})dv \\
&+ \int_{topcomposite} \rho_f(z)(\dot{u}\delta\dot{u} + \dot{w}\delta\dot{w})dv \\
&+ \int_{core} \rho_c(z)(\dot{u}\delta\dot{u} + \dot{w}\delta\dot{w})dv \\
&+ \int_{\substack{bottom\\composite}} \rho_f(z)(\dot{u}\delta\dot{u} + \dot{w}\delta\dot{w})dv \\
&+ \int_{\substack{bottom\\piezo}} \rho_p(z)(\dot{u}\delta\dot{u} + \dot{w}\delta\dot{w})dv
\end{aligned} \tag{43}$$

By applying Hamilton's principle and arranging the variables, the equations of motion are derived.

The boundary conditions for micro sandwich beam is obtained as follows:

$$\begin{aligned}
&\delta u_0 = 0 \qquad N_x = 0 \\
&\delta\phi = 0 \qquad M_x = 0, \qquad M_{xy}^{(0)} = 0 \\
&\delta w_0 = 0 \qquad Q_x = 0, \qquad \frac{\partial M_{xy}^{(0)}}{\partial x} = 0 \\
&\delta\frac{\partial w_0}{\partial x} = 0 \qquad M_{xy}^{(0)} = 0 \\
&\delta\psi = 0 \qquad D_x = 0, \\
&\int \frac{\partial(D_z\delta\psi)}{\partial z}dz = 0 \\
&\delta\Gamma = 0 \qquad B_x = 0, \\
&\int \frac{\partial(B_z\delta\Gamma)}{\partial z}dz = 0
\end{aligned} \tag{44}$$

where

$$\begin{aligned}
N_x &= \int \sigma_{xx}\,dz \\
M_x &= \int \sigma_{xx} z\,dz \\
Q_x &= \int \tau_{xz}\,dz \\
M_{xy}^{(0)} &= \int m_{xy}\,dz
\end{aligned} \tag{45}$$

3. Solving procedure

Assuming that the boundary conditions are simply supported in both ends of micro sandwich beam subjected to electric and magnetic fields, Navier's type solution can be used to solve the equations of motion as follows:

$$\begin{aligned}
u_0(x,t) &= \sum_{n=1}^{N} U_n cos\left(\frac{n\pi x}{l}\right)e^{-i\omega t}, \\
w_0(x,t) &= \sum_{n=1}^{N} W_n sin\left(\frac{n\pi x}{l}\right)e^{-i\omega t} \\
\phi(x,t) &= \textstyle\sum_{n=1}^{N} \Phi_n cos\left(\frac{n\pi x}{l}\right)e^{-i\omega t}, \\
E(x,t) &= \sum_{n=1}^{N} E_n sin\left(\frac{n\pi x}{l}\right)e^{-i\omega t} \\
M(x,t) &= \sum_{n=1}^{N} M_n sin\left(\frac{n\pi x}{l}\right)e^{-i\omega t}
\end{aligned} \tag{46}$$

where ω is vibration frequency.

By substituting the normal and shear stresses and modified couple stress in Eq. (45), and then the results in Eq. (44), it can be seen that the Navier's type solution is satisfied the boundary conditions.

The stiffness matrix and mass matrix using the governing equations of motion are derived as follows:

$$([K] - \omega^2[M])q = 0 \tag{47}$$

where K and M are stiffness and mass matrices, respectively, and $q = \{U_n \;\; W_n \;\; \Phi_n \;\; M_n \;\; E_n\}$ is an unknown vector corresponding to five unknown functions.

The parameter γ in stiffness matrix is a function of transverse deflection in mid-surface of micro beam. Note that parameters K_1 and K_2, which are required to determine transverse deflection, depend on the parameter γ. Therefore, the transverse deflection and the shape

Table 2 Comparison of natural frequencies of sandwich beam

mode		$V_{CNT}=0.12$		$V_{CNT}=0.17$		$V_{CNT}=0.28$	
	CNT Dist	Present	Wu *et al*. (2015)	Present	Wu *et al*. (2015)	Present	Wu *et al*. (2015)
1	UD	0.1375	0.1432	0.1497	0.1560	0.1715	0.1785
	FG	0.1395	0.1453	0.1527	0.1588	0.1755	0.1825
2	UD	0.5424	0.5650	0.5905	0.6140	0.6724	0.6997
	FG	0.5501	0.5730	0.5998	0.6247	0.6861	0.7147
3	UD	1.1949	1.2429	1.2939	1.3465	1.4636	1.5246
	FG	1.2095	1.2599	1.3152	1.3689	1.4909	1.5554

function s(z) are coupled to each other. Since the value of γ is not known a priori, an iterative technique is used. The iterative method is outlined as the following steps:

(1) Initializeγ, for instance, $\gamma = 1$
(2) Determine shape function by using Eq. (33)
(3) Solve equation of motions
(4) Determine the corresponding transverse deflection
(5) Calculate the new value of γ from Eq. (34).
(6) Repeat steps 1–5 until the difference between the ith and $(i+1)$ th values of γ

is less than a specified tolerance.

4. Discussion of results

In order to obtain a deep insight into the dynamic behavior of a micro sandwich beam subjected to electrical and magnetic potential resting on silica aerogel foundation, the variation of natural frequencies versus porosity distribution, porosity coefficient, volume fraction of CNT, electrical field, magnetic field, temperature and moisture effects and geometric parameters are studied in this section through free vibration analysis of the system.

4.1 Validation of vibration

In this study can be verified by imposing some specific restricted conditions on the equation-s and comparing the resultant equations with those of the previous studies. Two examples concerning the linear free vibration of sandwich beams and free vibration of micro beam are used to validate the present analysis through comparisons between the obtained results in this research and the existing ones.

The linear free vibration of sandwich beams is considered in Table 2 with a homogeneous core and composite face sheets reinforced by FG and uniformly CNT distribution. Material properties of composite face sheets are derived by the rule of mixture method, and it is assumed that volume fraction of CNT varies linearly along the thickness direction as follows:

$$V_{CNT}=\frac{(2z-h_c)}{h_f}V*\rightarrow(forbottomfacelayer) \tag{48}$$

$$V_{CNT}=\frac{(2z+h_c)}{-h_f}V*\rightarrow(fortopfacelayer) \tag{49}$$

where $V*=0.12$ and CNT efficiency parameter is $\eta_1=0.137$ in a case that CNT is uniformly distributed $V*=V_{CNT}$.

Table 3 Characterization data of beam Ma *et al*. (2008)

E	$1.44(GPa)$
υ	0.38
l_m	$17.6(\mu m)$
ρ	$1.22(10^3)(Kg/m^3)$
L	$20(H)$

Material constants of core and face sheets are Young's modulus, mass density and Poisson's ratio of homogeneous core (Ti-6Al-4V) are $E_{core}=113.8(GPa)$, $\rho_{core}=4430(kg/m^3)$ and $\nu_{core}=0.342$, respectively. Material properties of composite face layers are $E_m=2.5(GPa)$, $E_{CNT}=5.6466(TPa)$, $\rho_m=1190(kg/m^3)$ and $\rho_{CNT}=1400(kg/m^3)$, where 'm' and 'CNT' indicate matrix and carbon nanotube, respectively. Poisson's ratio of matrix material and CNT are $\nu_m=0.3$ and $\nu_{CNT}=0.175$, respectively.

Table 2 illustrates comparison of dimensionless natural frequencies of sandwich beam with composite face sheets. As can be observed, the dimensionless natural frequencies are in good agreement with results by Wu *et al*. (2015)

Another verification is carried out for free vibration of a micro Timoshenko beam and it is shown in Fig. 2, Ma *et al*. (2008). The material parameter and geometry properties of this micro beam are given in Table 3.

It can be found that dimensionless frequencies calculated by MCST have good agreement with the references results, especially in higher thickness to material parameter $(\frac{H}{l_m})$ ratio in Fig. 2.

Wu *et al*. (2015) considered sandwich beam with homogeneous core and composite reinforced by CNT while in the present work a micro sandwich beam composing of five layers such as two nanocomposites reinforced by carbon nanotubes layers, functionally graded porous core and two piezomagnetic/piezoelectric layers subjected to magneto electrical loadings. Thus this difference between two works is the maximum 4 percentage.

4.2 Numerical results

This section is devoted to study the effect of different parameters including porosity distribution along thickness direction, CNT distribution pattern, electric and magnetic fields, geometric parameters and temperature and moisture changes on the vibration behavior of micro sandwich beam subjected to electrical and magnetic fields resting on silica

Table 4 Material properties of core

E	$113.8(GPa)$
υ	0.342
ρ	$4430(Kg/m^3)$
L	$20(H)$

Table 5 Material properties of CNT and PMMA

E_{cnt}	5.6466 (TPa)
E_{PMMA}	2.5 (GPa)
υ_{cnt}	0.175
υ_{PMMA}	0.3
ρ_{CNT}	1190 (Kg/m$^{3)}$
ρ_{PMMA}	1400 (Kg/m$^{3)}$

Table 6 Material properties of silica aerogel

$E_{foundation}$	$9.368(10^{-7}) \times \rho_{foundation}^{3.378}$
$\upsilon_{foundation}$	$0.3236(\rho_{foundation}^{-0.107})$
$\rho_{foundation}$	$300 - 1000(Kg/m^3)$

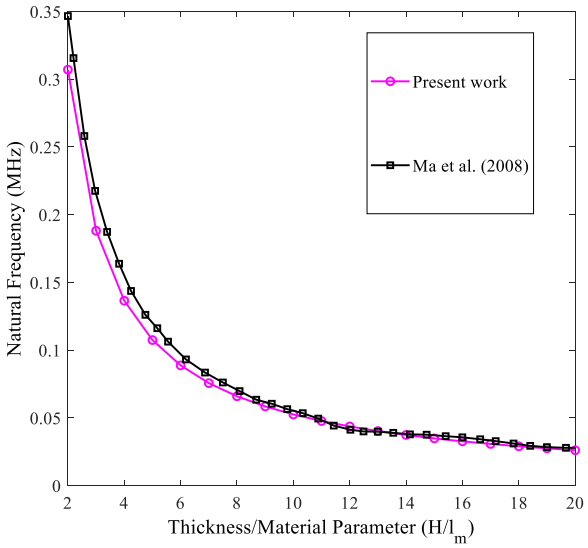

Fig. 2 Natural frequency varying with beam thickness

aerogel foundation with simply supported boundary conditions. Porous core of sandwich micro beam is made of Titanium alloy (Ti-6Al-4V) and its material and geometric properties are shown in Table 4.

Composite layers are made of poly methyl methacrylate reinforced by carbon nanotube. Table 5 indicates material constants of CNT and PMMA as follows:

Material properties of silica aerogel are considered by Arani and Zamani (2019) in Table 6.

For Figs. 3-14, the aspect ratio, thickness ratio, total thickness to material length scale parameter are assumed as follows: $\frac{L}{H} = 20, \frac{h_c}{h_f} = 8, H = 5(l_m)$.

Fig. 3. displays the relations between the porosity coefficient and dimensionless natural frequency for various porous distributions of the core which are uniform, symmetry and asymmetry. The figure shows that dimensionless natural frequency is greatly affected by porosity

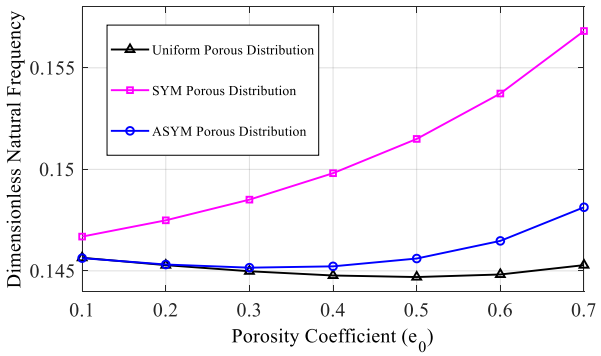

Fig. 3 The influence of porosity coefficient on dimensionless natural frequency for different porous distributions

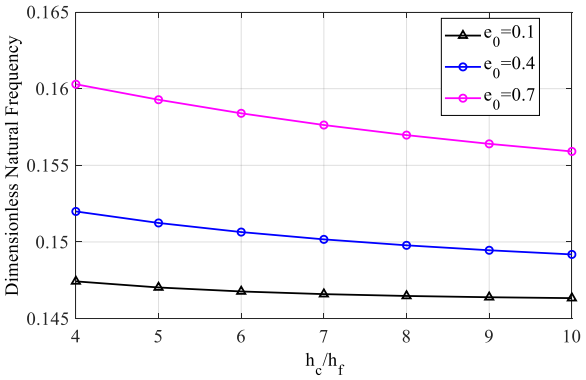

Fig. 4 The influence of h_c/h_f ratio and porosity coefficient on dimensionless natural frequency (L/H=20, H=5l_{lm})

coefficient. As seen from the figure, an increase in porosity coefficient leads to increase the natural frequency and porosity coefficient has a higher influence on symmetry porous distribution than asymmetry and uniform distributions. According to Fig. 1, this figure shows three porous distributions such as distribution 1 (symmetric distribution), distribution 2 (asymmetric distribution) and distribution 3 (uniform distribution). It is seen from Fig. 1 that the holes at the farthest distance from the neutral axes for symmetrical distribution are smaller than the other two states, so the stiffness of this case is more than the other two states and thus its frequency is higher than them. The holes for the uniform porous and ASYM distributions is more than SYM distribution. Thus this effect for mass matrix is more than stiffness matrix until 0.6 as well as 0.4 for the uniform porous and ASYM distributions, then in this range, the natural frequency decreases while, after e_0=0.6, the effect of stiffness matrix is higher than the mass matrix for the uniform porous and ASYM distributions, thus the natural frequency increases.

Fig. 4 depicts the variation of $\frac{h_c}{h_f}$ for three different porosity coefficients. It should be noticed that the total thickness of the micro sandwich beam is constant. The results are presented for symmetry distribution of porous core. It is obvious for all porosity coefficients that increasing the $\frac{h_c}{h_f}$ ratio will cause a decrease in the dimensionless natural frequency of the micro sandwich

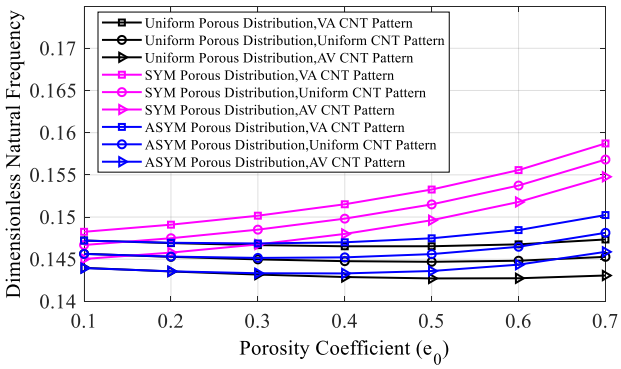

Fig. 5 The influence of porous distribution and CNT distribution pattern on dimensionless natural frequency (L/H=20, H=5l_{lm})

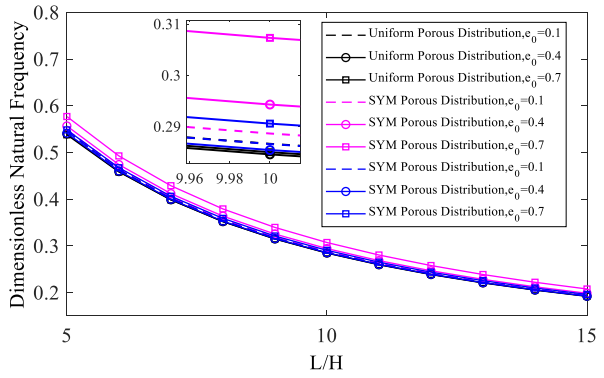

Fig. 6 Effect of aspect ratio on dimensionless natural frequency for different porous distributions and porosity coefficients (h_c/h_f=8)

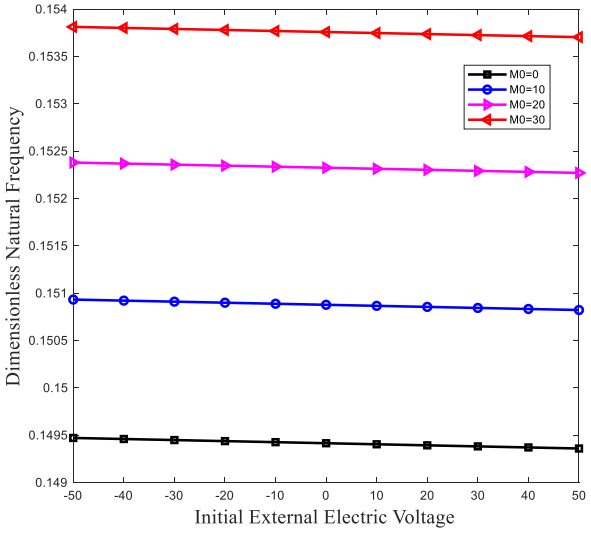

Fig. 7 The influence of initial external electric voltage on dimensionless natural frequency (L/H=20, H=5l_{lm})

beam. This means that by increasing core thickness and decreasing thickness of composite face layers at the same time, the stiffness of the micro sandwich beam reduces and result in a decrease in dimensionless natural frequency. On the other hands, with an enhance in the $\frac{h_c}{h_f}$ ratio, the micro

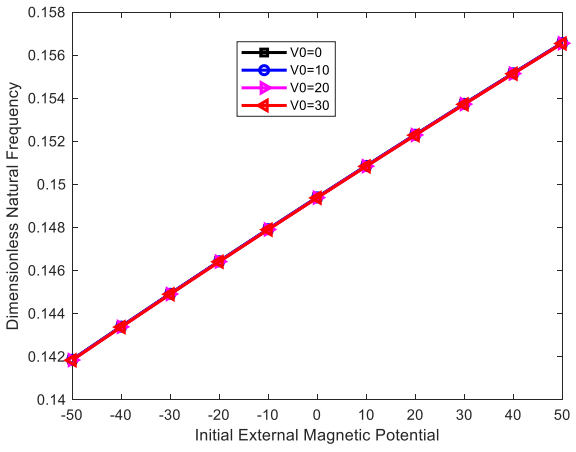

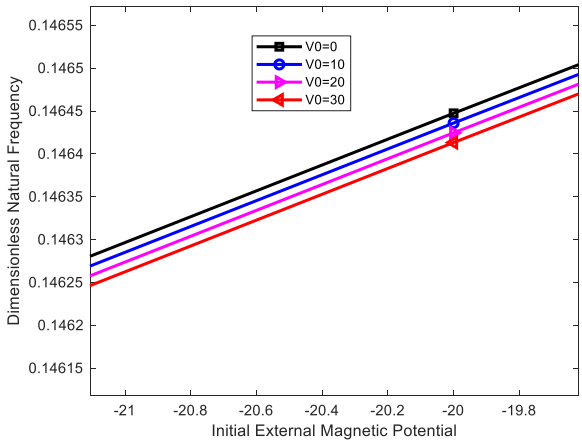

Fig. 8 The influence of initial external magnetic potential on dimensionless natural frequency (L/H=20, H=5l_{lm})

structure becomes more flexible, and then the stiffness of this structure reduces.

Fig. 5 shows the dimensionless natural frequency of micro sandwich beam versus porosity coefficient for various CNT distribution pattern and porous distribution. It is found that the VA CNT pattern in thickness direction provides a higher dimensionless natural frequency rather than uniform CNT pattern and AV CNT pattern. It can be found that the VA CNT pattern at the farthest distance from the neutral axes has more CNT at this edge, thus the stiffness of micro structure in this case increases with the other patterns.

The natural frequency of the micro sandwich beam with symmetry porosity distribution of core versus aspect ratio is plotted for three different porous distributions and porosity coefficients in Fig. 6. It is clear that with the increase of aspect ratio, the natural frequency decreases. As illustrated in the same porosity coefficient, symmetry porous distribution provides higher natural frequency. The holes at the farthest distance from the neutral axes for symmetrical distribution in Fig. 1 are smaller than the other two states, so the stiffness of this case is more than the other two states and thus its frequency is higher than them, thus the dimension of natural frequency for SYM porous distribution is more than two other cases.

The influence of initial external electric voltage for various initial external magnetic potential on the variation

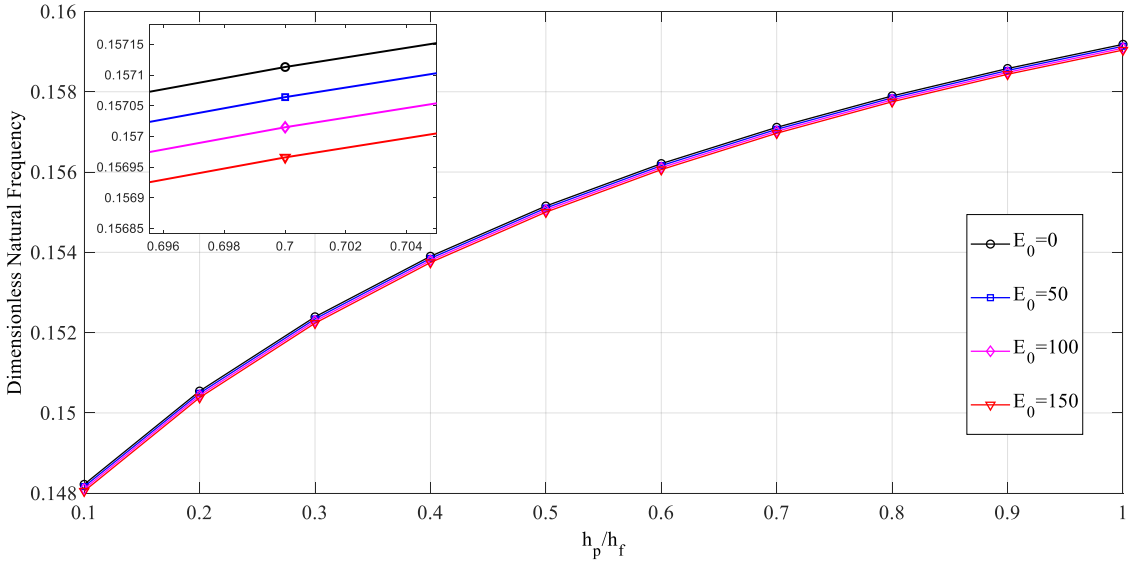

Fig. 9 Effect of h_p/h_f ratio on dimensionless natural frequency (L/H=20, H=5l_{lm})

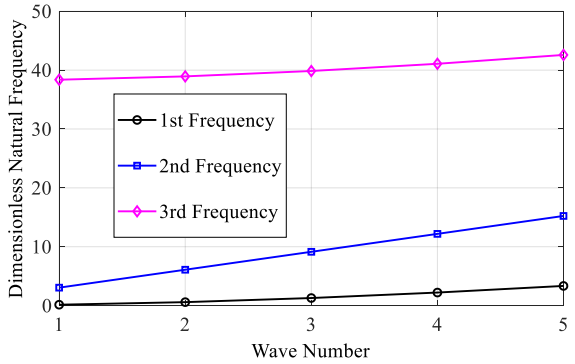

Fig. 10 Effect of wave number on dimensionless natural frequency (L/H=20, H=5l_{lm})

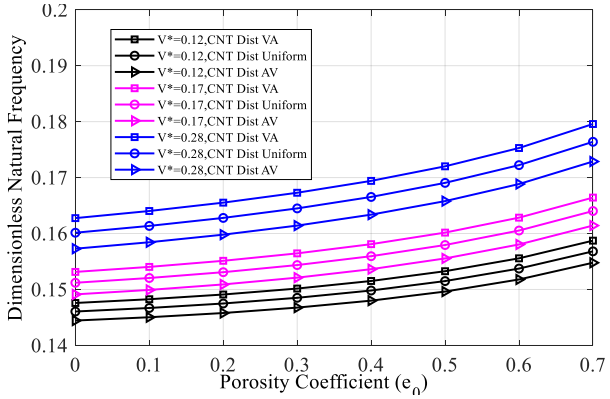

Fig. 11 Influence of CNT volume fraction and CNT pattern on dimensionless natural frequency (L/H=20, H=5l_{lm})

of the dimensionless natural frequency of the micro sandwich beam is presented in Fig. 7. It shows that increasing the initial external magnetic potential leads to enhance dimensionless natural frequency, increasing positive voltage at piezoelectric structure leads to create tensile axial force, thus the stiffness of micro structure increases.

Fig. 8 illustrates the effect of initial external magnetic potential on the dimensionless natural frequency. The results show that increasing initial magnetic potential leads to an increase in the dimensionless natural frequency. Also, it is observed that higher external voltage provides a less natural frequency of the micro sandwich beam. It shows that increasing the initial external electric voltage leads to reduce dimensionless natural frequency, increasing positive voltage at piezoelectric structure leads to create compressive axial force, thus the stiffness of micro structure decreases.

In Fig. 9, the changes in frequencies of the micro sandwich beams with different external loadings are presented in relation to the increase of h_p / h_f from 0.1 to 1. By increasing the h_p / h_f ratio, the dimensionless natural frequency increases. On the other hands, increasing the h_p / h_f ratio leads to increase the stiffness of micro structure. It should be mentioned that the total thickness of the micro sandwich beam is constant.

Fig. 10 shows the increasing dimensionless natural frequencies of micro sandwich beam due to the increase of wave number. As can be seen wave number increase each natural frequency.

Fig. 11 presents the effect of CNT volume fraction and CNT distribution pattern. One can found that no matter what CNT pattern is, the dimensionless natural frequency always increases by increasing of the CNT volume fraction. The VA CNT distribution pattern has higher dimensionless natural frequencies than that of the AV and uniform ones since the VA pattern provides higher stiffness of composite layers among the three. It can be found that the VA CNT pattern at the farthest distance from the neutral axes has more CNT at this edge, thus the stiffness of micro structure in this case increases with the other patterns. Also, increasing the volume fraction of CNT leads to increase the stiffness of micro structure and then enhances the dimensionless natural frequency.

Figs. 12 and 13 depict the effect of temperature rise and moisture on vibration behavior of micro sandwich beam.

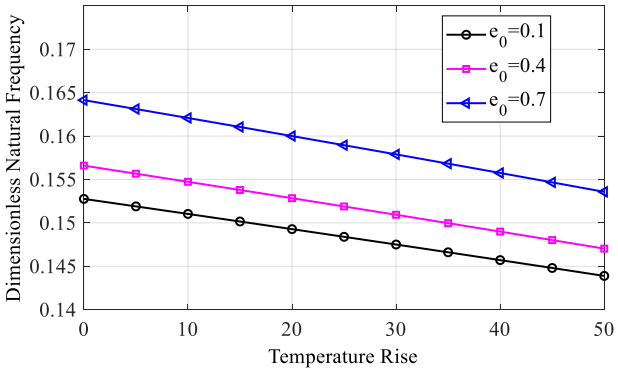

Fig. 12 Effect of temperature rises on dimensionless natural frequency for different porosity coefficient (L/H=20, H=5l_{lm})

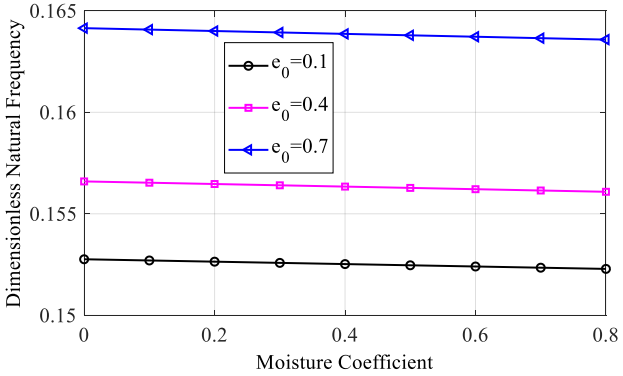

Fig. 13 The effect of moisture coefficient on dimensionless natural frequency for different porosity coefficient (L/H=20, H=5l_{lm})

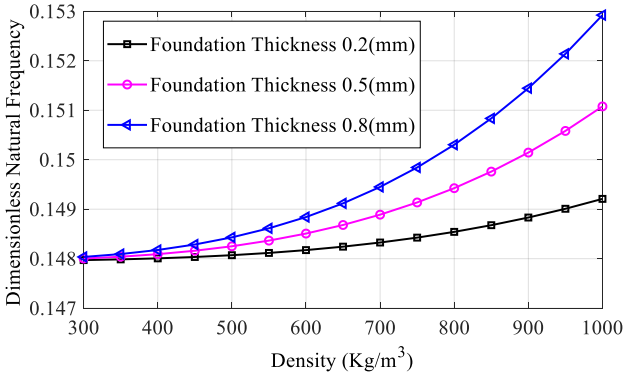

Fig. 14 Influence of density of foundation and thickness of foundation on dimensionless natural frequency (L/H=20, H=5l_{lm})

According to Fig. 12. The temperature change has a significant effect on the stiffness of the structure and a higher temperature rise leads to a decrease in the dimensionless natural frequency. Moisture also decrease the stiffness of microbeam and it leads to a less natural frequency.

In Fig. 14, the changes in frequencies of micro sandwich beam versus density of foundation is presented. It is apparent that the dimensionless natural frequency increases considerably as the increases of the density of foundation. It can be concluded that the thickness of foundation has a significant effect on vibration behavior of the micro sandwich beam. It is found that with increasing the thickness of foundation, the flexural rigidity of micro structure increases, and then the dimensionless natural frequency increases.

5. Conclusions

In this paper, the free vibration behavior of the micro sandwich beam composing of five layers such as functionally graded (FG) porous core, two nanocomposites reinforced by carbon nanotubes (CNTs) layers and two piezomagnetic/piezoelectric layers subjected to magneto electrical potential resting on silica aerogel foundation is investigated on the basis of the Timoshenko beam theory. The effect of foundation has been taken into account using Vlasov model in addition to rigid base assumption. For this purpose, an iterative technique is applied. The governing equations of the micro sandwich beam are derived in the Hamilton system. Navier's solution is established to analyze the free vibration of simply supported micro sandwich beam and is verified by comparing the available data. The natural frequencies are analyzed with different parameters including porous coefficient, porosity distribution, CNT volume fraction and CNT distribution pattern, geometric parameters, temperature and moisture effect.

The results of this paper may be summarized as follows:

1. The results show porosity coefficient plays an important role on the vibrational behaviors. Increasing porosity coefficient leads to an increase in the dimensionless natural frequency and porosity coefficient has more effect on symmetric porous distribution than asymmetric and uniform porous distribution.

2. The aspect ratio has significant effects on the dimensionless natural frequencies. The increase aspect ratio can decrease the stiffness of the structure, which leads to decrease of the dimensionless natural frequencies.

3. CNT distribution pattern through the thickness of composite layers has a significant effect on dimensionless natural frequencies. The maximum stiffness occurs when the composite layers have VA distribution. Because this distribution of CNTs in the composite layers increases the bending stiffness at top and bottom of cross section.

4. The foundation material and geometrical characteristics have remarkable effects on vibration behavior of micro sandwich beam. By the increase of density of silica Aerogel foundation, dimensionless natural frequency is increased. Also, the height of the silica Aerogel foundation has the same effect as density.

5. Temperature and moisture change of the micro sandwich beam have a small effect on dimensionless natural frequencies. Increasing temperature and moisture change lead to decrease the stiffness of the micro beam, which reduces dimensionless natural frequency.

6. Initial external magnetic potential and initial external electric voltage have a slight effect on dimensionless natural frequency. By increasing initial external magnetic potential dimensionless natural frequency increases but initial external electric voltage has a vice versa effect on vibration

behavior of the micro sandwich beam.

Thus if the authors want to increase only the stiffness of structure, then they can be used the nano particle of piezomagnetic/piezoelectric in resin of nanocomposite. Thus in this case, it should be considered 3 layers such as functionally graded (FG) porous core, nanocomposite reinforced by carbon nanotubes (CNTs) as well as nano particle of piezomagnetic/piezoelectric. Actually and in applicable, we consider sandwich structure with three layers such as functionally graded (FG) porous core, nanocomposite reinforced by carbon nanotubes (CNTs) that for control these structures, the authors have been considered the top and bottom layers in sandwich structures piezomagnetic/piezoelectric layers induced by magneto electrical potential that using these layers, we control the amplitude of vibration. This idea is considered in this work that it will follow in the feature work entitled "Active control of magneto electro micro sandwich beam with FG porous core".

Acknowledgments

The authors would like to thank the reviewers for their valuable comments and suggestions to improve the clarity of this work. Also, they would like to thank the Iranian Nanotechnology Development Committee for their financial support and the University of Kashan for supporting this work by Grant No. 682561/24.

References

Akbaş, Ş.D, (2017), "Forced vibration analysis of functionally graded porous deep beams", *Compos*. *Struct*., **186**, 293-302. https://doi.org/10.1016/j.compstruct.2017.12.013

Akhavanalavi, S.M., Mohammadimehr, M., Edjtahed, S.H. (2019), "Active control of micro Reddy beam integrated with functionally graded nanocomposite sensor and actuator based on linear quadratic regulator method", *Eur*. *J*. *Mech*. *A Solids*, **74**, 449-461. https://doi.org/10.1016/j.euromechsol.2018.12.008

Al-shujairi, M., Mollamahmutoğlu, Ç. (2018), "Buckling and free vibration analysis of functionally graded sandwich micro beams resting on elastic foundation by using nonlocal strain gradient theory in conjunction with higher order shear theories under thermal effect", *Compos*. *Part B Eng*., **154**, 292-312. https://doi.org/10.1016/j.compositesb.2018.08.103

Ansari, R., Norouzzadeh, A., Shakouri, A.H., Bazdid-vahdati, M., Rouhi, H. (2017), "Thin-Walled Structures Finite element analysis of vibrating micro beams and -plates using a three-dimensional micropolar element", *Thin Wall*. *Struct*., **124**, 489-500. https://doi.org/10.1016/j.tws.2017.12.036

Arani, A.G. and Kiani, F. (2018), "Nonlinear free and forced vibration analysis of microbeams resting on the nonlinear orthotropic visco-Pasternak foundation with different boundary conditions", *Steel Compos. Struct*., **28**(2), 149-165. https://doi.org/10.12989/scs.2018.28.2.149

Arani, A.G., Zamani, M.H. (2019), "Investigation of electric field effect on size- dependent bending analysis of functionally graded porous shear and normal deformable sandwich nanoplate on silica Aerogel foundation", *J*. *Sandw*. *Struct*. *Mater*., **21**(8), 2700-2734. https://doi.org/10.1177/1099636217721405

Arefi, M., Karroubi, R., Irani-Rahaghi, M. (2016), "Free vibration analysis of functionally graded laminated sandwich cylindrical shells integrated with piezoelectric layers", *Appl*. *Math. Mech*., **37**(7), 821-834. https://doi.org/10.1007/s10483-016-2098-9

Arefi, M., Pourjamshidian, M., Arani, A.G. (2018), "Free vibration analysis of a piezoelectric curved sandwich nano-beam with FG-CNTRCs face-sheets based on various high-order shear deformation and nonlocal elasticity theories", *Eur*. *Phys*. *J*. *Plus*., **133**(5), 193. https://doi.org/10.1140/epjp/i2018-12015-1

Arefi, M. and Zenkour, A.M. (2017), "Vibration and bending analysis of a sandwich microbeam with two integrated piezo-magnetic face-sheets", *Compos*. *Struct*., **159**, 479-490. https://doi.org/10.1016/j.compstruct.2016.09.088

Bamdad, M., Mohammadimehr, M., Alambeigi, K. (2020). "Bending and buckling analysis of sandwich Reddy beam considering shape memory alloy wires and porosity resting on Vlasov's foundation", *Steel Compos*. *Struct*., **36**(6), 671-687. https://doi.org/10.12989/scs.2020.36.6.671

Bahaadini, R., Saidi, A.R. (2018), "On the stability of spinning thin-walled porous beams", *Thin Wall*. *Struct*., **132**, 604-615. https://doi.org/10.1016/j.tws.2018.09.022

Chan, D.Q., Van Thanh, N., Khoa, N.D., Duc, N.D. (2020), "Nonlinear dynamic analysis of piezoelectric functionally graded porous truncated conical panel in thermal environments", *Thin Wall*. *Struct*., **154**, 106837. https://doi.org/10.1016/j.tws.2020.106837

Chen, D., Yang, J., Kitipornchai, S. (2017) "Nonlinear vibration and postbuckling of functionally graded graphene reinforced porous nanocomposite beams", *Compos*. *Sci*. *Technol*., **142**, 235-245. https://doi.org/10.1016/j.compscitech.2017.02.008.

Chen, D., Yang, J., Kitipornchai, S. (2016a) "Nonlinear free vibration of shear deformable sandwich beam with a functionally graded porous core", *Thin Wall*. *Struct*., **197**, 39-48. https://doi.org/10.1016/j.tws.2016.05.025.

Chen, D., Yang, J., Kitipornchai, S. (2016b), "Free and forced vibrations of shear deformable functionally graded porous beams", *Int*. *J*. *Mech*. *Sci*. **108-109**, 14-22. https://doi.org/10.1016/j.ijmecsci.2016.01.025.

Dastjerdi, S., Abbasi, M. (2018), "A vibration analysis of a cracked micro-cantilever in an atomic force microscope by using transfer matrix method", *Ultramicroscopy*., **196**, 33-39. https://doi.org/10.1016/j.ultramic.2018.09.014

Dat, N.D., Quan, T.Q., Mahesh, V., Duc, N.D. (2020), "Analytical solutions for nonlinear magneto-electro-elastic vibration of smart sandwich plate with carbon nanotube reinforced nanocomposite core in hygrothermal environment", *Int*. *J*. *Mech*. *Sci*., **186**, 105906. https://doi.org/10.1016/j.ijmecsci.2020.105906

De, Souza., Eloy, F., Gomes, G.F., Ancelotti, J.r, A.C., Da, Cunha., J.r, S.S., Bombard, A.J., Junqueira, D.M. (2018), "Experimental dynamic analysis of composite sandwich beams with magnetorheological honeycomb core", *Eng*. *Struct*., **176**, 231-242. https://doi.org/10.1016/j.engstruct.2018.08.101

Domagalski, Ł. (2018), "Free and forced large amplitude vibrations of periodically inhomogeneous slender beams*", Arch*. *Civil Mech*. *Eng*., **18**(4), 1506-1519.

Duc, N.D., Van Tung, H. (2010), "Nonlinear analysis of stability for functionally graded cylindrical panels under axial compression", *Comput*. *Mater*. *Sci*., **49**(4), S313-S316. https://doi.org/10.1016/j.commatsci.2009.12.030

Duc, N.D. (2014), *Nonlinear Static and Dynamic Stability of Functionally Graded Plates and Shells*, Vietnam: Vietnam Natl Univ Press.

Duc, N.D. (2016a), "Nonlinear thermal dynamic analysis of eccentrically stiffened S-FGM circular cylindrical shells surrounded on elastic foundations using the Reddy's third-order shear deformation shell theory", *Eur*. *J*. *Mech*. *A Solids*, **58**, 10-30. https://doi.org/10.1016/j.euromechsol.2016.01.004

Duc, N.D. (2016b), "Nonlinear thermo-electro-mechanical dynamic

response of shear deformable piezoelectric sigmoid functionally graded sandwich circular cylindrical shells on elastic foundations", *J. Sandw. Struct. Mater*, **20**(3), 351-378. https://doi.org/10.1177/1099636216653266

Duc, N.D., Quan, T.Q. (2014), "Transient responses of functionally graded double curved shallow shells with temperature-dependent material properties in thermal environment", *Eur. J. Mech. A Solids*, **47**, 101-123. https://doi.org/10.1016/j.euromechsol.2014.03.002

Duc, N.D., Pham, C.H. (2018), "'Nonlinear dynamic response and vibration of sandwich composite plates with negative Poisson's ratio in auxetic honeycombs", *J. San. Struct. Mater*., **20**(6), 692-717. https:// 10.1177/1099636216674729.

Ebrahimi, F., Barati, M.R. (2018), "Hygro-thermal vibration analysis of bilayer graphene sheet system via nonlocal strain gradient plate theory", *J. Brazil. Soc. Mech. Sci. Eng*., **40**(9), 428-435. https://doi.org/10.1007/s40430-018-1350-y

Eltaher, M.A., Fouda, N., El-midany, T., Sadoun, A.M. (2018), "Modified porosity model in analysis of functionally graded porous nanobeams", *J. Brazil. Soc. Mech. Sci. Eng*., **40**(3), 141-149. https://doi.org/10.1007/s40430-018-1065-0

Khdeir, A.A., Aldraihem, O.J. (2016), "Free vibration of sandwich beams with soft core", *Compos. Struct*., **154**, 179-189. https://doi.org/10.1016/j.compstruct.2016.07.045

Kiarasi, F., Babaei, M., Mollaei, S., Mohammadi, M., Asemi, K. (2021). "Free vibration analysis of FG porous joined truncated conical-cylindrical shell reinforced by graphene platelets", *Adv. Nano Res*., **11(4),** 361-380. https://doi.org/10.12989/anr.2021.11.4.361

Kim, J., Żur, K.K., Reddy, J.N. (2018), "Bending, free vibration, and buckling of modified couples stress-based functionally graded porous micro-plates", *Compos. Struct*., **209**, 879-888. https://doi.org/10.1016/j.compstruct.2018.11.023

Kitipornchai, S., Chen, D., Yang, J. (2016), "Free vibration and elastic buckling of functionally graded porous beams reinforced by graphene platelets", *Mater. Des*., **116**, 656-665. https://doi.org/10.1016/j.matdes.2016.12.061

Khoa, N.D., Thiem, H.T., Duc, N.D. (2019), "Nonlinear buckling and postbuckling of imperfect piezoelectric S-FGM circular cylindrical shells with metal–ceramic–metal layers in thermal environment using Reddy's third-order shear deformation shell theory", *Mech. Adv. Mater. Struct.*, **26**(3), 248-259. https://doi.org/10.1080/15376494.2017.1341583

Li, L., Tang, H., Hu, Y. (2017), "Size-dependent nonlinear vibration of beam-type porous materials with an initial geometrical curvature", *Compos. Struct*., **184**, 1177-1188. https://doi.org/10.1016/j.compstruct.2017.10.052

Liu, H., Liu, H., Yang, J. (2018), "Vibration of FG magneto-electro-viscoelastic porous nanobeams on visco-Pasternak foundation", *Compos. Part B Eng*., **155**, 244-256. https://doi.org/10.1016/j.compositesb.2018.08.042

Luat, D. T., Van Thom, D., Thanh, T. T., Van Minh, P., Van Ke, T., Van Vinh, P. (2021). "Mechanical analysis of bi-functionally graded sandwich nanobeams", *Adv. Nano Res*., **11**(1), 55-71. https://doi.org/10.12989/anr.2021.11.1.055

Long, N.V., Nguyen, V.L., Tran, M.T., Thai, D.K. (2022) "Exact solution for nonlinear static behaviors of functionally graded beams with porosities resting on elastic foundation using neutral surface concept ", *Proc. Inst. Mech. Eng. Part C J. Mech. Eng. Sci*., **236**(1), 481-495. https://doi.org/10.1177/09544062211021112.

Madenci, E. (2021). "Free vibration analysis of carbon nanotube RC nanobeams with variational approaches", *Adv. Nano Res*., **11**(2), 157-171. https://doi.org/10.12989/anr.2021.11.2.157

Ma, H.M., Gao, X.Ã., Reddy, J.N. (2008), "Journal of the mechanics and physics of solids a microstructure-dependent Timoshenko beam model based on a modified couple stress theory", *J. Mech. Phys. Solids*., **56**(12), 3379-3391. https://doi.org/10.1016/j.jmps.2008.09.007

Mirjavadi, S.S., Afshari, B.M., Shafiei, N., Rabby, S., Kazemi, M. (2018), "Effect of temperature and porosity on the vibration behavior of two-dimensional functionally graded micro scale Timoshenko beam", *J. Vib. Control*., **24**(18), 4211-4225. https://doi.org/10.1177/1077546317721871

Mohammadimehr, M., Akhavan, Alavi, S., Okhravi, S., Edjtahed, S. (2017), "Free vibration analysis of micro- magneto-electro-elastic cylindrical sandwich panel considering functionally graded carbon nanotube – reinforced nanocomposite face sheets, various circuit boundary conditions , and temperature-dependent material properti", *J. Intell. Mater. Syst. Struct*., **29**(5), 863-882. https://doi.org/10.1177/1045389X17721048

Mohammadimehr, M., Mohammadi-Dehabadi, A.A., Akhavan, Alavi, S.M., Alambeigi, K., Bamdad, M., Yazdani, R., Hanifehlou, S. (2018), "Bending, buckling, and free vibration analyses of carbon nanotube reinforced composite beams and experimental tensile test to obtain the mechanical properties of nanocomposite", *Steel Compos. Struct*., **29**(3), 405-422. https://doi.org/10.12989/scs.2018.29.3.405

Mohammadimehr, M., Okhravi, S.V., Alavi, S.M.A. (2016a), "Free vibration analysis of magneto-electro-elastic cylindrical composite panel reinforced by various distributions of CNTs with considering open and closed circuits boundary conditions based on FSDT", *J. Vib. Control*., **24**(8), 1551-1569. https://doi.org/10.1177/1077546316664022

Mohammadimehr, M., Salemi, M., Navi, B.R. (2016b), "Bending, buckling, and free vibration analysis of MSGT microcomposite Reddy plate reinforced by FG-SWCNTs with temperature-dependent material properties under hydro-thermo-mechanical loadings using DQM", *Compos. Struct*., **138**, 361-380. https://doi.org/10.1016/j.compstruct.2015.11.055

Nejadi, M. M., Mohammadimehr, M. (2020). "Buckling analysis of nanocomposite sandwich Euler-Bernoulli beam considering porosity distribution on elastic foundation using DQM". *Adv. Nano Res*., **8(1)**, 59-68. https://doi.org/10.12989/anr.2020.8.1.059

Nejadi, M. M., Mohammadimehr, M., Mehrabi, M. (2021). "Free vibration and buckling of functionally graded carbon nanotubes/ graphene platelets Timoshenko sandwich beam resting on variable elastic foundation", *Adv. Nano Res*., **10**(6), 539-548. https://doi.org/10.12989/anr.2021.10.6.539

Nguyen, T.B., Reddy, J.N., Rungamornrat, J., Lawongkerd, J. (2019) "Nonlinear analysis for bending, buckling and post-buckling of nano-beams with nonlocal and surface energy effects", *Int. J. Struct. Stabil. Dyn*., **19**(11), 1950130. https://doi.org/10.1142/S021945541950130X

Quan, T.Q., Dinh Duc, N. (2016), "Nonlinear vibration and dynamic response of shear deformable imperfect functionally graded double-curved shallow shells resting on elastic foundations in thermal environments", *J. Therm. Stress*., **39**(4), 437-459. https://doi.org/10.1080/01495739.2016.1158601

Quan, T.Q., Van Quyen, N., Duc, N.D. (2021), "An analytical approach for nonlinear thermo-electro-elastic forced vibration of piezoelectric penta–Graphene plates", *Eur. J. Mech. A Solids*, **85**, 104095. https://doi.org/10.1016/j.euromechsol.2020.104095

Quan, T.Q., Anh, V.M., Mahesh, V., Duc, N.D. (2020). "Vibration and nonlinear dynamic response of imperfect sandwich piezoelectric auxetic plate", *Mech. Adv. Mater. Struct*., 1-11. https://doi.org/10.1080/15376494.2020.1752864

Safari, M., Mohammadimehr, M., Ashrafi, H. (2021), "Free vibration of electro-magneto-thermo sandwich Timoshenko beam made of porous core and GPLRC", *Adv. Nano Res*., **10**(2), 115-128. https://doi.org/10.12989/anr.2021.10.2.115

Sahmani,, S., Mohammadi, M., Rabczuk, T. (2018), "Nonlocal strain gradient plate model for nonlinear large-amplitude

vibrations of functionally graded porous micro / nano-plates reinforced with", *Compos. Struct.*, **198**, 51-62. https://doi.org/10.1016/j.compstruct.2018.05.031

Sadeghpour, E., Sadighi, M., Ohadi, A. (2015), "Free vibration analysis of a debonded curved sandwich beam", *Eur. J. Mech. A Solids.*, **57**, 71-84. https://doi.org/10.1016/j.euromechsol.2015.11.006

Safari, M., Mohammadimehr, M., Ashrafi, H. (2023), "'Forced vibration of a sandwich Timoshenko beam made of GPLRC and porous core", *Struct. Eng. Mech.*, **88**(1), 1-12. https://doi.org/10.12989/sem.2023.88.1.001

Sae-Long, W., Limkatanyu, S., Hansapinyo, C., Prachasaree, W., Rungamornrat, J., Kwon, M. (2021a) "Nonlinear flexibility-based beam element on Winkler-Pasternak foundation", *Geomech. Eng.*, **24**(4), 371-388. https://doi.org/10.12989/gae.2021.24.4.371

Sae-Long, W., Limkatanyu, S., Rungamornrat, J., Prachasaree, W., Sukontasukkul, P., Sedighi, H.M. (2021b) "A rational beam-elastic substrate model with incorporation of beam-bulk nonlocality and surface-free energy", *Eur. Phys. J. Plus*, **136**(1), 80. https://doi.org/10.1140/epjp/s13360-020-00992-7

She, G., Ren, Y., Yuan, F., Xiao, W. (2018), "On vibrations of porous nanotubes", *Int. J. Eng. Sci.*, **125**, 23-35. https://doi.org/10.1016/j.ijengsci.2017.12.009

Şimşek, M., Al-shujairi, M. (2016), "Static, free and forced vibration of functionally graded (FG) sandwich beams excited by two successive moving harmonic loads", *Compos. Part B Eng.*, **108**, 18-34. https://doi.org/10.1016/j.compositesb.2016.09.098

Tian, J., Zhang, Z., Hua, H. (2018), "Free vibration analysis of rotating functionally graded double-tapered beam including porosities", *Int. J. Mech. Sci.*, **150**, 526-538. https://doi.org/10.1016/j.ijmecsci.2018.10.056

Tossapanon, P., Wattanasakulpong, N. (2016), "Stability and free vibration of functionally graded sandwich beams resting on two-parameter elastic foundation", *Compos. Struct.*, **142**, 215-225. https://doi.org/10.1016/j.compstruct.2016.01.085

Tran, M.T., Nguyen V.L., Pham, S.D., Rungamornrat, J. (2020) "Free vibration of stiffened functionally graded circular cylindrical shell resting on Winkler–Pasternak foundation with different boundary conditions under thermal environment", *Acta Mechanica*, **231**(6), 2545-2564. https://doi.org/10.1007/s00707-020-02658-y

Vo, D., Duong, N.H., Rungamornrat, J., Nanakorn, P. (2022a) "A 2D field-consistent beam element for large displacement analysis using a rational Bézier representation with varying weights", *Appl. Math. Model.*, **104**, 806-825. https://doi.org/10.1016/j.apm.2021.12.022.

Vo, D., Zhou, K., Rungamornrat, J., Bui, T.Q. (2022b) "Spatial arbitrarily curved microbeams with the modified couple stress theory: Formulation of equations of motion", *Eur. J. Mech. A Solids*, **92**, 104475. https://doi.org/10.1016/j.euromechsol.2021.104475.

Walczak, Z., Jasion, P., Wittenbeck, L. (2017), "Buckling and vibrations of metal sandwich beams with trapezoidal corrugated cores – the lengthwise corrugated main core", *Thin Wall. Struct.*, **112**, 78-82. https://doi.org/10.1016/j.tws.2016.12.013

Wang, Y., Xie, K., Fu, T., Shi, C. (2018), "Vibration response of a functionally graded graphene nanoplatelet reinforced composite beam under two successive moving masses", *Compos. Struct.*, **209**, 928-939. https://doi.org/10.1016/j.compstruct.2018.11.014

Wu, H., Kitipornchai, S., Yang, J. (2015), "Free vibration and buckling analysis of sandwich beams with functionally graded carbon nanotube-reinforced", *Int. J. Struct. Stabil. Dyn.*, **15**(7), 1540011. https://doi.org/10.1142/S0219455415400118

Wu, H., Yang, J., Kitipornchai, S. (2020) "Mechanical analysis of functionally graded porous structures: A review", *Int. J. Struct. Stabil. Dyn.*, **20**(13), 2041015. https://doi.org/10.1142/S0219455420410151.

Xue, Y., Jin, G., Ma, X., Chen, H., Ye, T., Chen, M., Zhang, Y. (2019), "Free vibration analysis of porous plates with porosity distributions in the thickness and in-plane directions using isogeometric approach", *Int. J. Mech. Sci.*, **52**, 346-362. https://doi.org/10.1016/j.ijmecsci.2019.01.004

Zeng, S., Wang, B.L., Wang, K.F. (2018), "Nonlinear vibration of piezoelectric sandwich nanoplate with a functionally graded porous core with consideration of flexoelectric effect", *Compos. Struct.*, **207**, 340-351. https://doi.org/10.1016/j.compstruct.2018.09.040

Zhang, K., Ge, M., Zhao, C., Deng, Z., Xu, X. (2018), "Free vibration of nonlocal Timoshenko beams made of functionally graded materials by Symplectic method", *Compos. Part B Eng.*, **156**, 174-184. https://doi.org/10.1016/j.compositesb.2018.08.051

Zhang, Z., Han, B., Zhang, Q., Jin, F. (2017), "Free vibration analysis of sandwich beams with honeycomb-corrugation hybrid cores", *Compos. Struct.*, **171**, 335-344. https://doi.org/10.1016/j.compstruct.2017.03.045

Zhu, K., Chung, J. (2019), "Vibration and stability analysis of a simply-supported Rayleigh beam with spinning and axial motions", *Appl. Math. Modell.*, **66**, 362-382. https://doi.org/10.1016/j.apm.2018.09.021

AT